

Testing the omnigenic model for a behavioral trait in *Drosophila melanogaster*

Wenyu Zhang, R. Guy Reeves, Diethard Tautz#

Address for all authors:

Department of Evolutionary Genetics, Max Planck Institute for Evolutionary Biology, 24306 Plön,
Germany

#corresponding author:

Email: tautz@evolbio.mpg.de

Phone: +49 4522763390

Running title: Omnigenic network for pupation behaviour

Key words: *Drosophila melanogaster*, behaviour, pupation, automated phenotyping, DGRP lines, genome
wide association mapping, genetic network, omnigenic model

Abstract

The omnigenic model suggests the existence of core networks of genes for quantitative traits, which are influenced by modifiers that may encompass most, if not all expressed genes in the genome. We have studied pupation site choice behaviour in *Drosophila* to test this model. Based on a GWA analysis of the *Drosophila* Genetic Reference Panel (DGRP) stocks, we identify candidate genes and show for disrupted versions of the genes that most are indeed involved in the phenotype. These candidate genes also allowed us to identify a core network and we experimentally confirm the involvement of other members of this core network in the trait. Intriguingly, when randomly choosing 20 non-network genes we also find an involvement in the trait for most of them. Comparison of phenotypic effect sizes suggest that the core network genes have on average stronger effects. Our data thus confirm the predictions of an omnigenic genetic architecture.

Introduction

Organismal phenotypes, *i.e.* traits measured in whole organisms usually have a quantitative distribution and their genetic architecture can be studied by genome wide analysis (GWA) approaches. In the past years, these approaches have revealed that such phenotypes have a polygenic architecture in the sense that many genes of moderate or small effect contribute to the phenotype. The in depth analysis of the extensive data collected in the framework of the studies on human height have shown that the general practice to use a genome wide statistical significance cut-off to declare loci being involved in a phenotype leave most of the heritability of the trait unaccounted for (Wood et al., 2014; Yang et al., 2011, 2010). Hence, the attention has turned towards the loci falling below this cut-off. A study focussing on these small effect loci has suggested that all, or at least almost all, genes can be expected to contribute to the phenotype. This has led to the suggestion of an omnigenic model for quantitative traits (Boyle et al., 2017; Liu et al., 2019). It assumes that there is a set of core genes forming pathways with special relevance for the phenotype, or disease etiology in human disease studies. These are expected to be modified by many, if not all other genes expressed in the same cells. Although the effect sizes of these other genes are expected to be smaller than those of the core genes, in sum they explain more of the genetic variance or heritability than the set of core genes. However, an explicit test of this model is still lacking.

We assess here predictions of the omnigenic model using an ecologically relevant quantitative behavioural trait in *Drosophila melanogaster*, namely pupation site choice. The pupal stage is a life history stage found in holometabolous insects undergoing transformation between larval and adult stages (Jones and Reiter, 1975; Price, 1970). The choice of pupation site is known to directly influence the probability of successful eclosion of adult flies (Joshi and Mueller, 1993; Rodriguez et al., 1992; Sokolowski, 1985), as pupae are exposed to many biotic and abiotic risks while immobilized during the 3-4 days of metamorphosis. Patterns of pupation site choices in a number of *Drosophila* species have been extensively investigated (Erezyilmaz and Stern, 2013; Markow, 1979; Vandal et al., 2012, 2008), and substantial variation has been found both within and between species. Several environmental factors, such as temperature (Schnebel and Grossfield, 1992), light (Markow, 1981; Schnebel and Grossfield, 1986), humidity (Casares et al., 1997; Sokal et al., 1960) and food medium (Harini, 2013; Hodge and Caslaw, 1998) have been shown to contribute to the variation. Biotic factors were also identified, including sex (Casares and Carracedo, 1987), larval development time (Welbergen and Sokolowski 1994), and larval density in the vial (Joshi and Mueller, 1993; Sokolowski and Hansell, 1983).

Previous genetic association studies to explore the genetic basis of pupation site choice in *Drosophila* were consistent with it being a complex behavioural trait with a polygenic basis (Erezyilmaz and Stern, 2013; Riedl et al., 2007; Sharon J. Bauer and, 1985; Sokolowski and Bauer, 1989). However, although there have been multiple studies on this trait and its genetics, they were so far hampered by limited sample size, as well as limited genetic resolution. We adapted here an automated method for pupal phenotyping (Reeves and Tautz, 2017) to determine the genetics of

pupation height choice, while controlling for environmental factors. The automated phenotyping allows analysis of large numbers of pupae, maximising the potential to reach statistical significance even for small effect sizes.

For assessing the genetic contribution to this behavioural trait, we use the extensive genetic resources available for *Drosophila*. This includes the *Drosophila* Genetic Reference Panel (DGRP) as a resource for association mapping, as well as the gene disruption lines maintained at the Bloomington *Drosophila* Stock Centre (BDSC).

The DGRP consists of a population of more than 200 highly inbred *Drosophila melanogaster* strains derived from a wild population (Huang et al., 2014; MacKay et al., 2012), which has been successfully applied to identify the association between a broad range of phenotypes and their underlying genetic basis (Dembeck et al., 2015; Durham et al., 2014; Huang et al., 2014), including several behavioural traits (Lee et al., 2017; Rohde et al., 2017; Shorter et al., 2015; Xue et al., 2017). Together with the well-resolved richness in genetic polymorphisms and rapid decay in linkage disequilibrium (LD) in these strains (Huang et al., 2014), these make the DGRP a great panel to study the genetic basis of pupation height choice in *Drosophila melanogaster* at a fine scale resolution. A potential drawback of the lines is that they are limited in number, implying that genetic effect sizes of specific loci need to be large enough to be captured with a genome-wide significance threshold. However, as indicated above, it has become increasingly clear that the use of such a threshold is too stringent anyway. The efforts to avoid false positive associations by such thresholds are blocking the way towards understanding the genetic networks underlying a complex trait. An alternative approach is therefore to use lower statistical thresholds and to combine this with a direct test of the candidate genes that are uncovered in this way. The BDSC gene disruption lines cover almost all genes of *Drosophila* and can therefore be used to test most of GWA candidate genes for a possible involvement in the trait.

In the present study, we go beyond a standard GWA combined with experimental gene confirmation, in order to explore two further aspects. First, we ask what the candidate genes reveal on the possible core network of the trait and then further use genes from the predicted network to test them for their effects. Second, following the predictions of the omnigenic model, we explore also the effects of genes randomly chosen among genes expressed in the respective life stage. We find that not only a large fraction of the network predicted genes, but also of the randomly chosen genes have an effect on the pupation height phenotype, whereby the phenotypic effect sizes of the core network genes are higher than those of the randomly chosen genes. We conclude that these findings support predictions of an omnigenic genetic architecture for quantitative traits.

Results

Phenotyping

The acquisition of phenotype data from a large number of individuals is a prerequisite for high resolution genetic mapping studies. Instead of using the mostly manual measurement based approach from previous studies on pupation height (Erezyilmaz and Stern, 2013; Riedl et al., 2007; Sharon J. Bauer and, 1985; Sokolowski and Bauer, 1989), we adapted an earlier image-analysis based phenotyping pipeline (Reeves and Tautz, 2017). This pipeline was initially developed for the high-throughput measurement of pupal case length, and was shown to have the capability for the automatic detection of pupae with a high precision (Reeves and Tautz, 2017). We modified it for the purpose of the measurement of pupation height choice, defined as the distance from the vertical coordinate of pupation site (pupal center) to the food surface in the vial in millimetre (mm). Figure 1 shows an example of the automated measurement of pupation height.

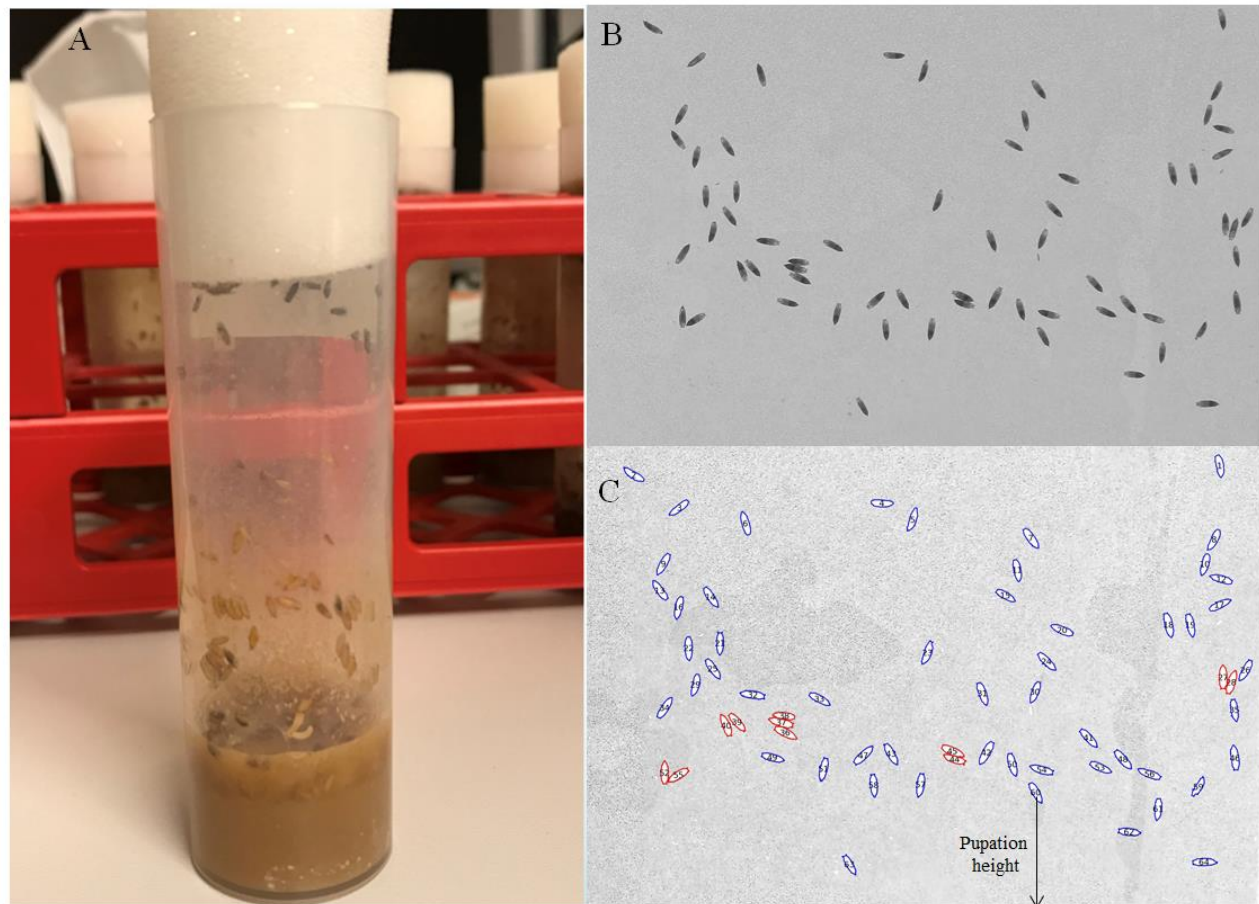


Figure 1: Automated measurement of pupation height. (A) The pupae in the vial crawl up the wall for pupation. The vial includes a plastic sheet that lines the wall. This is taken out after a sufficient number of pupae are attached and it is photographed (B). The image analysis software CellProfiler (Carpenter et al., 2006) is then used to identify the outlines of the pupae (C) and to identify single ones that can be reliably measured (marked in blue). After optimizing the system, we achieve accuracy for pupae detection of around 99.85%, with only a small fraction of loss of true positive results (< 0.7%).

Density of individuals within the vial in which they develop is a common major environmental covariate of many *Drosophila* traits, including pupation site choice (Joshi and Mueller, 1993; Sokolowski and Hansell, 1983). In the present study, individual density variation was controlled in an indirect manner through limiting the number of parents used per vial (10 females for wildtype strains, and 15 females for inbred strains), and restricting the number of nights they remained before being removed (1-2 nights). Still, some variation was apparent that required to be addressed. Based on a set of test experiments, we defined minimal sampling rules of at least 15 measured pupae per vial and at least six replicate vials per strain. Further, in order to minimize the influence of individual density within vials, an average slope (0.145) across all tested stocks was used to correct the mean estimate of pupation height in all vials.

Variation in pupation height

Two distinct sets of strains were used to explore the variance in pupation height choice. The first dataset consisted of 14 natural wild-type *Drosophila melanogaster* strains collected from different parts of the world (Supplementary file 1A). The second dataset was from the *Drosophila* Genetic Reference Panel (DGRP) (Huang et al., 2014; MacKay et

al., 2012) and included 198 lines (Supplementary file 1B). In order to correct for environmental factors, especially cryptic differences in humidity (Casares et al., 1997; Sokal et al., 1960), two wildtype stocks (S-317 and S-314) representing two extremes of pupation height from the first strain set and showing a consistent trend, were continually re-measured to act as controls throughout all experiments. The estimates of pupation height for the strains were corrected based on the average pupation height of the two control stocks across all rounds of experiments.

Figure 2 shows the profiles of corrected pupation height from the wildtype and DGRP sets of strains. We observe large variation of pupation height among strains, ranging from pupation height of only 15 mm above the food medium up to the very highest possible position adjacent to the plug surface of the vial (50 mm). The global wildtype lines showed no obvious geographical clustering of pupation heights. The spread of pupation height among the DGRP stocks exceeds that of the wildtype stocks, suggesting that they capture at least a major part of the existing variation in *D. melanogaster*.

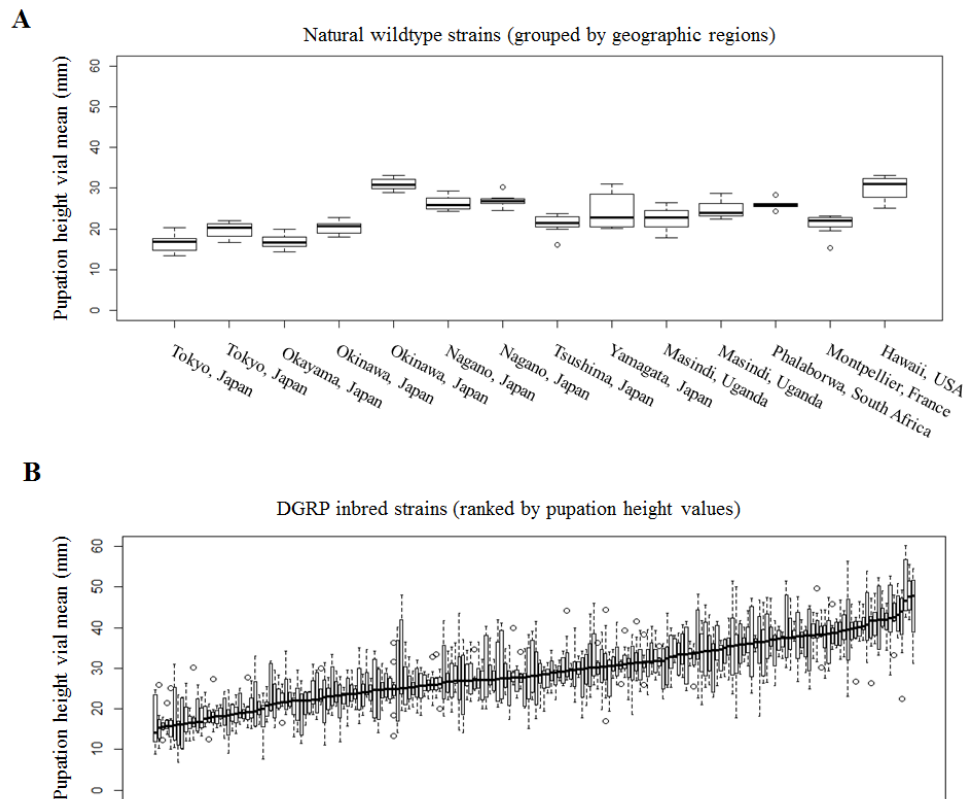


Figure 2: Distribution of pupation height for different strains. (A) Natural global stocks and (B) DGRP inbred strains (B). At least 6 vial measurement (vial pupae density ≥ 15) were conducted for each stock. On average, 7.8 vial measurements (530 individual pupae) and 8.2 vial measurements (335 individual pupae) were examined for each strain from the wildtype and DGRP inbred stocks, respectively.

Sexual dimorphism and parental effects

Sexual dimorphism, the condition where sexes from the same species exhibit different characteristics for morphological or behavioural traits, is a commonly observed phenomenon. Regarding the pupation site choice in *Drosophila*, a controversy on the existence of sexual dimorphism has persisted for several decades. Early studies have reported no sex dimorphism on pupation site choice in *Drosophila* (Markow, 1979; Sokolowski and Bauer,

1989; Welbergen and Sokolowski, 1994), while the results from other studies showed that males pupated significantly higher than females (Casares and Carracedo, 1987; Riedl et al., 2007).

To address the sexual dimorphism question, a distinct dataset incorporating both pupation height and sex information of more than 4,000 randomly selected (2,340 females and 1,935 males) individuals from 728 vials generated from the 4-way pedigree dataset reported by (Reeves and Tautz, 2017) was analysed. Since this earlier study had not recorded the level of the food surface, the pupation height for each sexed pupae was calculated as the deviation from the corresponding vial (on which the pupae locates) to average pupation height (Figure 3A) (Reeves and Tautz, 2017). As shown in Figure 3B, there was a significant difference in pupation height between males and females (Wilcoxon rank sum test: P -value $1.5E-07$), with male individuals pupating on average around 2 mm higher than females. This result is roughly in line with the observed sexual dimorphism reported in two previous studies (Casares and Carracedo, 1987; Riedl et al., 2007). The difference in pupation site choice between the sexes may be due to their distinct developmental timing, as females generally pupate later than males, and later larvae tend to pupate lower, possibly due to a response to diminishing levels of humidity inside the vials (Casares and Carracedo, 1987).

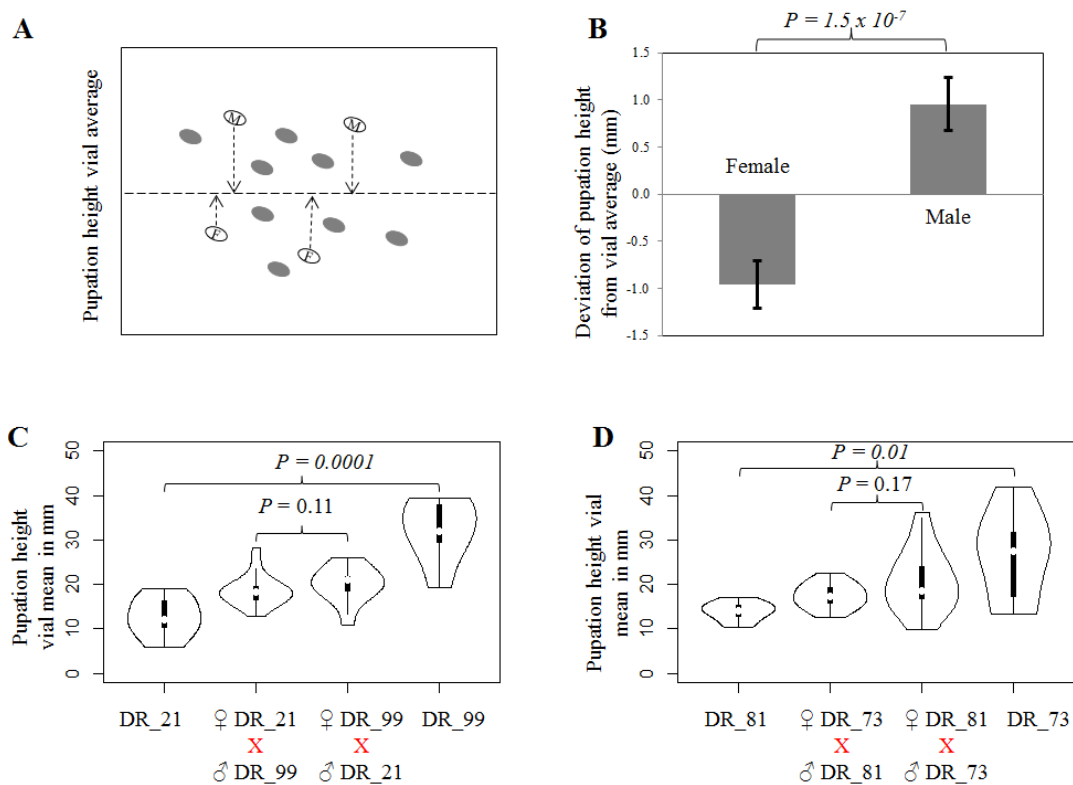


Figure 3: Sex dimorphism and parental bias for pupation height in *Drosophila melanogaster*. (A) Shows a scheme with pupae on the film surface and explains how the deviation on pupation height of sexed individuals compared to the vial mean values; (B) Shows the distribution of the deviation of pupation height from vial mean in mm for sexed pupae. The error bars indicate the standard error of mean values. Two pairs of DGRP inbred lines, (C) DR_21 and DR_99, (D) DG_81 and DR_73, with each pair representing two extremes of pupation height choice status were reciprocally crossed to test for significantly phenotypic differences with the parental stocks. The significance P -values were computed with Wilcoxon rank sum test.

Figure 3 - figure supplement 1: Comparison of pupation height status between *Wolbachia*-free and *Wolbachia*-infected stocks.

Figure 3 – figure supplement 2: Experimental test of *Wolbachia* infection effect on pupation height.

A parental bias, by which the phenotype of an individual depends more upon the mother's or father's phenotype or genotype, can be observed for some traits. This can be the result of inheritance of genetic material in the cytoplasm (e.g., mitochondria, *Wolbachia* bacteria), sex chromosomes, or imprinted gene regions. Previous studies on this aspect for pupation site selection provided two opposing views, with one suggesting the pupation site choice in *Drosophila* fits a simple additive model of inheritance without any parental bias (Sokolowski and Bauer, 1989), while the others found a significant maternal effect on pupation site selection (Garcia-Flores et al., 1989; Singh and Pandey, 1993). To address this question, two pairs of DGRP inbred lines with each pair representing two extremes of pupation height were randomly chosen, and were reciprocally crossed to test for parental biases. As shown in Figure 3C and 3D, the pupation heights for offspring from both directions lie between their parental stocks, with no significant differences (Wilcoxon rank sum test: *P*-values 0.11 and 0.17) on pupation height choice in reciprocal crosses. This finding supports the additive model of inheritance on pupation site selection in *Drosophila melanogaster* (Sokolowski and Bauer, 1989).

Wolbachia pipientis is a maternally transmitted endosymbiotic bacterium that infects around 53% of DGRP strains. It was reported to have a significant effect on some behavioural traits, e.g., acute and chronic resistance to oxidative stress (Huang et al., 2014). Two different approaches were used to explore a possible effect of *Wolbachia* infection on pupation height. First, the statistical analysis on the pupation height between all tested strains with infected and non-infected strains exhibited no significant difference of pupation height (Wilcoxon rank sum test: *P*-value 0.29, (Figure 3 - figure supplement 1). Second, the experimental phenotypic comparison between pupation height of three randomly selected DGRP strains with *Wolbachia* infection and those after the removal of *Wolbachia* using tetracycline treatment showed no significant statistical difference on pupation height choice for all tested strains (Figure 3 - figure supplement 2). Accordingly, the *Wolbachia* infection on DGRP strains was not incorporated in the association analysis below, as both the indirect and direct evidences described above reveal no strong effect on pupation height choice.

Heritability and chromosome effects

An estimate of the total genetic component of pupation height choice, i.e., broad sense heritability (H^2), was achieved by determining the proportion of total variance in the mean strain height measurements compared to the average within each strain (Schmidt et al., 2017). The additive genetic impact, or narrow sense heritability (h^2), is reported here as "SNP heritability" (Wray et al., 2013), i.e., the estimate of the proportion of phenotypic variance explained by all available SNPs (or genetic variants) in the DGRP stocks.

All estimates are shown in Table 1. Values of H^2 of 0.64 (0.70 for wildtype strains) and h^2 of 0.46 (SE: 0.2) based on the estimates from DGRP inbred stocks imply higher heritability than that from previous estimates within this species (Casares and Carracedo, 1986; Garcia-Flores et al., 1989; Singh and Pandey, 1993).

Table 1 Statistics for the estimation of the heritability of pupation height choice

Heritability	Dataset	Method	Covariates	Heritability Estimate
H^2	wildtype strains ^a	IBM SPSS (Variance component)	-	0.70
			Pupae density	0.71
H^2	DGRP inbred strains ^b	IBM SPSS (Variance component)	-	0.64
			Pupae density	0.64
h^2	DGRP inbred strains ^b	GEMMA univariate linear mixed model { V_G/V_P }	-	0.46 ± 0.20 SE

^aNumber of stocks = 14; Number of vials measured = 109; Mean replicates per IL= 7.8 ± 0.6 SD; Mean number of measured pupae per vial = 69 ± 24 SD

^bNumber of stocks = 198; Number of vials measured = 1627; Mean replicates per IL= 8.2 ± 1.6 SD; Mean number of measured pupae per vial = 40 ± 17 SD

Table 1 - table supplement 1: Distribution of the explained phenotypic variance for each chromosome based on chromosome size and number of genetic variants within each chromosome.

Partitioning the variance by chromosome reveals that all apart chromosome 4 contribute a substantial part to the variance of pupation height (Table 1 - table supplement1). The minimal contribution from chromosome 4 can be ascribed to the limited number of genetic variants within this chromosome. In line with previous reports (BAUER and SOKOLOWSKI 1985; Sokolowski and Bauer 1989), we find a somewhat higher contribution of autosomes to the variance of pupation height and also a slightly larger effect from chromosome 2 compared to chromosome 3 (Sharon J. Bauer and, 1985).

Genome-wide association analysis

The GWA analysis was based on the genetic variants of DGRP freeze 2 (Huang et al., 2014), variants with missing values above 20% and minor allele frequency below 5% were excluded from the further analysis. The linear regression model implemented in PLINK (Purcell et al., 2007) was used for the genome wide association analysis, including the assessments of possible covariates.

A previous study had shown a possible role of larval size on their pupation site choice (Vandal et al., 2012). Here we use pupal case length as an indicator of larval size (Reeves and Tautz, 2017). We find that there is indeed a weak, but significant negative correlation between pupal case length and pupation height (Figure 4 - figure supplement 1, panel A, Pearson's correlation test, R-square 0.02, P -value $3.7E-07$). Therefore, a second GWA was performed using pupation height as phenotype and pupal case length as covariate. This analysis revealed an extremely strong correlation between P -values of GWA with and without pupal case length as a covariate (Figure 4 - figure supplement 1, panel B, Pearson correlation test, R square 0.99, P -value $< 2.2E-16$) and no major difference in the q - q plots (Figure 4 - figure supplement 1, panels C and D). Based on these analyses, we conclude that the identified significant genetic variants on pupation height are mostly independent from its association with pupal case length.

To investigate whether any cryptic population structure could contribute to the observed variation in pupation site choice of inbred stocks, PLINK (Purcell et al., 2007) was used to identify major principal components (PC) of genetic variants in the DGRP strains. Only one major cluster was found in these stocks based on PC analysis (Huang et al., 2014), and no obvious clusters, within which the strains share the same pupation height (Figure 4 - figure supplement 2). Moreover, only three out of top 20 PCs showed significant (Pearson's correlation test, P -value <0.05) correlations with pupation height, while all of them can only explain low fractions (3% to 6%, based on R^2 values) of observed phenotypic variance (Figure 4 - figure supplement 3), for which the slight correlations seem more likely to come from a few outlier individuals.

Given their driving force on population divergence and speciation (Hoffmann and Rieseberg, 2008), major genomic inversions in DGRP strains might contribute to the observed population structure and the association between population structure and pupation height. The systematic test for the correlations between genomic inversion status in DGRP strains and the first two principal components of genomic variation showed significant effects only from In(2L)t and In(3R)Mo (Figure 4 - figure supplement 4), indicating their possible roles in population subdivisions (Hoffmann and Rieseberg, 2008). However, there is no significant association between pupation height and all tested genomic inversions, including In(2L)t and In(3R)Mo.

The original DGRP lines were constructed such that population structure effects should be minimized, but some genetic relatedness leading to cryptic population structure might still exist (Mackay and Huang, 2018). Hence, for identifying candidate loci, one could use different types of correction of population structure. While such corrections should reduce the number of false positive associations, they compromise also the power to detect true associations (Price et al., 2010). Hence, we decided to use the uncorrected data for a first list of candidate loci from which we chose genes for further functional analysis (Figure 4).

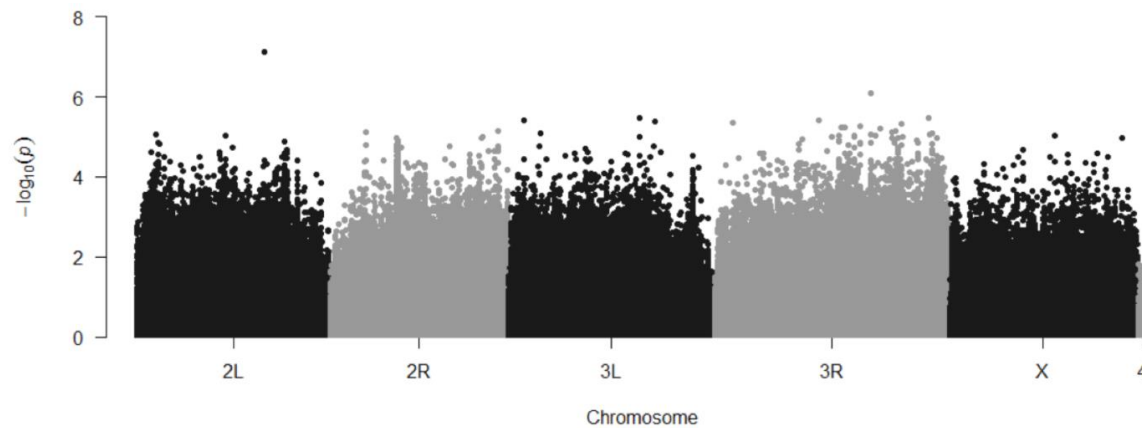


Figure 4: Manhattan plot for genome-wide association results for pupation height without covariate.

Figure 4 - figure supplement 1: Dependence of pupation height choice on pupal case size.

Figure 4 - figure supplement 2: Correlation between pupation height and population structure.

Figure 4 - figure supplement 3: Correlation between pupation height and top 20 PCs.

Figure 4 - figure supplement 4: Correlation between pupation height status and inversion status in DGRP strains.

Candidate genes from the GWA analysis

When using genome-wide permutation based thresholds (P -value $< 5E-08$, see Methods), we find no significant genetic variants associating with pupation height (Figure 4). We decided therefore to use the more permissive significance cut-off of P -value $< 1E-05$, which is a nominal threshold frequently used in *Drosophila* quantitative trait genetic studies (Lee et al., 2017). At this cut-off, we found 28 significant genetic variants (25 SNPs and 3 indels) to be associated with pupation height in the DGRP strains, corresponding to 71 associating genes that locate within 5kb up/down-stream (default setting in SnpEff (Cingolani et al., 2012)) of these genetic variants (Table 2).

To identify additional candidate genes associated with the variants, we examined the long range linkage disequilibrium (LD) between pairs of detected candidate variants and with other genetic variants found in the DGRP strains. No significant linkages between physically distant ($\geq 1\text{Mb}$, with $r^2 \geq 0.8$) genetic variants were found, suggesting the associations in this population are not confounded by long range LD. LD blocks were then calculated for each significant genetic variant with a commonly used threshold $r^2 = 0.8$ (Pallares et al., 2014), and 10 significant LD blocks were found with average block size of 5.3 kb (Table 2 – table supplement 1). No pairs of identified significant variants were found in the same LD block. This finding is in line with the observation of a rapid decay of LD in the panel strains reported in the original DGRP resource reference (Huang et al., 2014). Combining the additional genes identified in the above LD blocks, we identified in total 81 candidate genes associating with pupation height variation in *Drosophila melanogaster*. None of these identified candidate genes overlap with the previously reported pupation height association QTL at 56A01-C11 in (Riedl et al., 2007).

288 **Table 2: Genome-wide association results on pupation height**

Genetic variant	Minor allele frequency	GWA association p-value	Associating genes [#] (location)	lesion types / effect in genetic stocks tested	Tester (BDSC ID)	Progenitor (BDSC ID)
2L_15093153_SNP	0.33	7.59E-08	CG15270 (Intron)	DEL / *	25163	5905
3R_18609357_SNP	0.46	8.00E-07	CG7029 (Intron)	DEL / *	7671	6326
3L_15604180_SNP	0.24	3.40E-06	CG13449 (Exon); CG7650 (Upstream); RhoGAP71E,Comm3 (Downstream)	DEL / **	27888	6326
3R_25409303_SNP	0.39	3.45E-06	CG7567 (Downstream)	DEL / **	8925	5905
3R_12465747_SNP	0.06	3.75E-06	Arl6IP1,nonA-1 (Upstream); Fas I (Downstream)	DEL / n.s.	7737	6326
3L_1844225_SNP	0.11	3.96E-06	Cpr62Bc (Upstream)	DEL / n.s.	7567	6326
3L_17493227_SNP	0.08	4.14E-06	Oatp74D (Intron); Edin (Downstream)	DEL / *	7611	6326
3R_2131013_SNP	0.05	4.58E-06	Osi16(Exon);CG31560(Upstream);Osi14,Osi15,CG31556(Downstream)	-		
3R_22219289_SNP	0.08	4.82E-06	CG33970 ,ppk15(Intergenic)	INS / **	22850	5905
3R_17249156_DEL	0.26	5.33E-06	Lbl(Intron)	-		
3R_15464523_SNP	0.41	5.64E-06	Subdued(Intron);CG34138,Vha13(Downstream)	-		
3R_15083169_SNP	0.27	5.83E-06	CG14280(5'UTR)	-		
3R_19710692_SNP	0.21	6.23E-06	Pellino (Intron)	INS / n.s.	26071	5905
3R_21494031_SNP	0.13	7.10E-06	Lgr3(Intron);RASSF8(Downstream)	-		
2R_20001939_INS	0.09	7.23E-06	CG3253(5'UTR);CG4049,CG3257(Upstream)	-		
2R_4192787_SNP	0.11	7.74E-06	CG30371,pdm3(Intergenic)	-		
3R_21098010_SNP	0.07	7.79E-06	CG11891 (Exon);CG11878(Upstream);CG11859(Downstream);CG10513(Downstream)	INS / ***	26044	5905
3R_25865027_SNP	0.44	7.96E-06	janA(Exon);CG7928, Ocn ,janB,Sry-beta,Sry-alpha,Sry-delta(Upstream);Axn(Downstream)	INS / ***	15632	6599
3L_3881099_SNP	0.07	8.38E-06	Awh,Fie(Intergenic)	-		
3R_25643196_SNP	0.13	8.58E-06	CG7829(Exon);Vps16B,neo(Upstream);ca(Downstream)	-		
3R_18560721_SNP	0.10	8.70E-06	Dcr-1 (Exon);Takl2(Upstream);CG6982,CG17618(Downstream)	-		
2L_2261132_SNP	0.38	8.87E-06	CG4270, Send1 (Upstream);CG34049(Downstream)	INS / ***	16121	6326
3R_19152989_SNP	0.09	9.11E-06	Pnt(Intron)	-		
3R_16569860_SNP	0.29	9.12E-06	CG42322(Intron);CG31199(Upstream);CG31200,Pros28.1A(Downstream)	-		
3R_14797512_SNP	0.45	9.15E-06	CG42613 (Exon);CG43732(3'UTR)	INS / ***	29121	5905
X_12597625_SNP	0.06	9.31E-06	Smr (Intron);CG15725(Upstream)	INS / n.s.	26090	5905
2L_10535124_INS	0.14	9.47E-06	CG18302(Intron); Lip4 ,CG18301(Downstream)	INS / ***	24290	5905
3R_22370558_SNP	0.18	9.75E-06	Scribbled (Intron)	INS / *	17791	6326

289

290 **Note:** DEL = deletion line, INS = transposon insertion line, ***: P-value<0.001; **: P-value<0.01; *: P-value<0.05; n.s.: P-value>0.05; BDSC: Bloomington Drosophila Stock Centre; Highlighted in red are
291 the ones applied for phenotype confirmations. [#] associating genes are defined as those locate within 5kb up/down-stream of target genetic variant.

292 **Table 2 - table supplement 1:** LD regions for Genome-wide association results.

Phenotype confirmations

The advantage of *Drosophila* as a model system is that one can use mutant alleles that have been constructed in a common co-isogenic background to test whether different alleles in genes implicated by the GWA analyses indeed affect pupation site choice. Gene disruption lines were available for 16 candidate loci (with disruption in the coding region of at least 1 gene for each locus) within the 28 identified associated loci. Nine constitute transposon insertion mutations (Bellen et al., 2011) and seven constitute small deficiencies (Supplementary file 1C). Experimental tests generally involved replicated phenotypic comparisons between the co-isogenic progenitor stock and homozygous or heterozygous disruptions of the target genes (see Methods).

An overview on the measured pupation height differences compared to the respective progenitor stocks is provided in Figure 5. Twelve out of 16 tested candidate loci showed a significant difference, five with an increased height, and seven with a decreased one. The eight transposon insertion stocks that are homozygous viable (completely viable or semi-viable) show a decreased (*Smr*, *Scrib*, *Ocnus*, *Lip4* and *Send1*) or increased (*CG11891*, *CG42613*, and *Pellino*) pupation height, two of which only in tendency (Wilcoxon rank sum test, P-value >0.05).

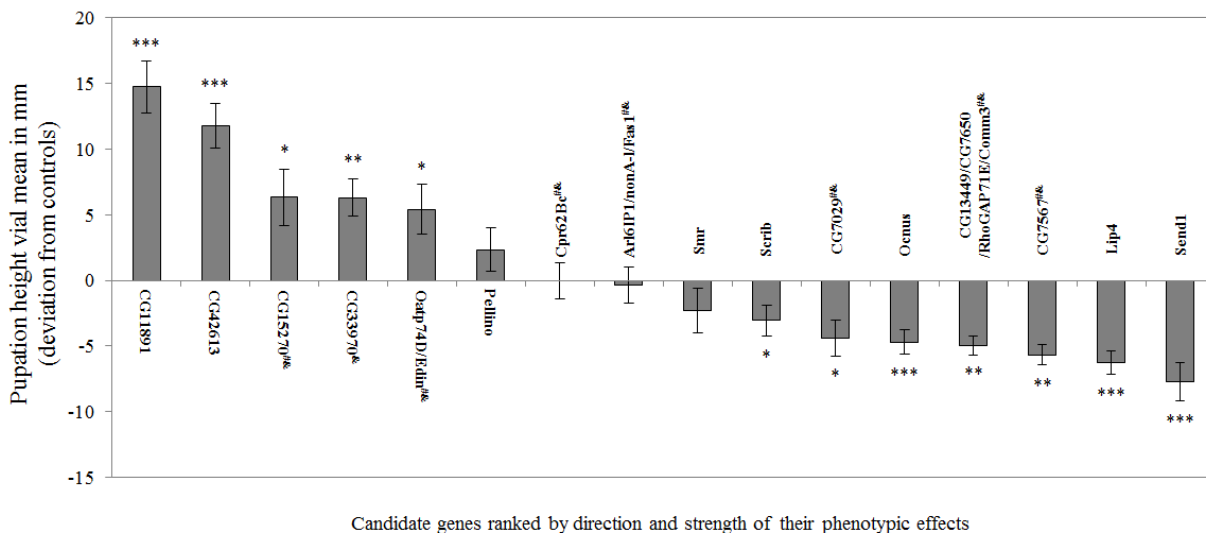


Figure 5: Phenotype effects of candidate genes from gene disruption test. The phenotypic effect was measurement as the deviation of pupation height of stocks with gene-disruption compared with that from progenitor stocks. The error bars show the standard error of mean values. ***: P-value < 0.001; **: P-value < 0.01; *: P-value < 0.05; # indicates deficiencies stocks, otherwise transposon insertion mutants; & indicates haplo-disruption stocks, otherwise homozygous-insertion mutants.

The other two stocks that show no significant overall change (Cp62Bc and Arl6IP1/nonA-I/Fas1) are deletion stocks that are homozygous lethal, i.e., the fact that we did not find an effect on pupation height in hemizygous state does not rule out the possibility that other alleles would show it. Two other homozygous deletion lethal strains (corresponding to genes CG7029 and Oatp74D/Edin) do show a significant influence on pupal height status, implying a haplo-insufficient or dominant effect. Four further homozygous lethal strains which could only be tested under conditions where 50% of the pupae should be hemizygotes (see Methods for details), (corresponding to one gene CG33970 from transposon insertion disruption, and three loci CG15270, CG13449/CG7650/RhoGAP71E/Comm3 and CG7567 from DNA segment deletion disruption) show significant effects as well, indicating a particularly strong haplo-insufficient or dominant effect. However, each of the deletions affects multiple genes (Supplementary file 1C), leaving it open whether another gene in the region causes the effect.

Expression and network analysis

Pupation follows the third instar larval (L3) stage in *Drosophila*. Hence, one can ask whether genes involved in pupation site choice are more likely to have a substantial expression at this stage, especially in the central nervous system, given that this is a behavioural phenotype. To test this hypothesis, the gene expression profiling data from the *Drosophila* modENCODE project (Brown et al., 2014) were explored, which measured the genome-wide gene expression for five tissues in L3 stages in *Drosophila melanogaster*, including central nervous system (CNS), digestive system, fat tissue, imaginal disc and salivary glands. As expected, larger fractions of expressed genes (RPKM > 0) for the identified candidate gene dataset among all tested tissues in L3 stages were found, compared with the expression profiling of total annotated protein-coding genes as controls (Figure 6A). We also find that the median expression levels of candidate genes compared to the randomly selected genes are significantly higher in the CNS (Wilcoxon rank sum test, P-value=0.006), but not other tissues (Figure 6B). This observation is consistent with the above prediction that the identified candidate genes for pupation site choice are enriched in the CNS of third instar larvae, where they could have a direct influence on behaviour.

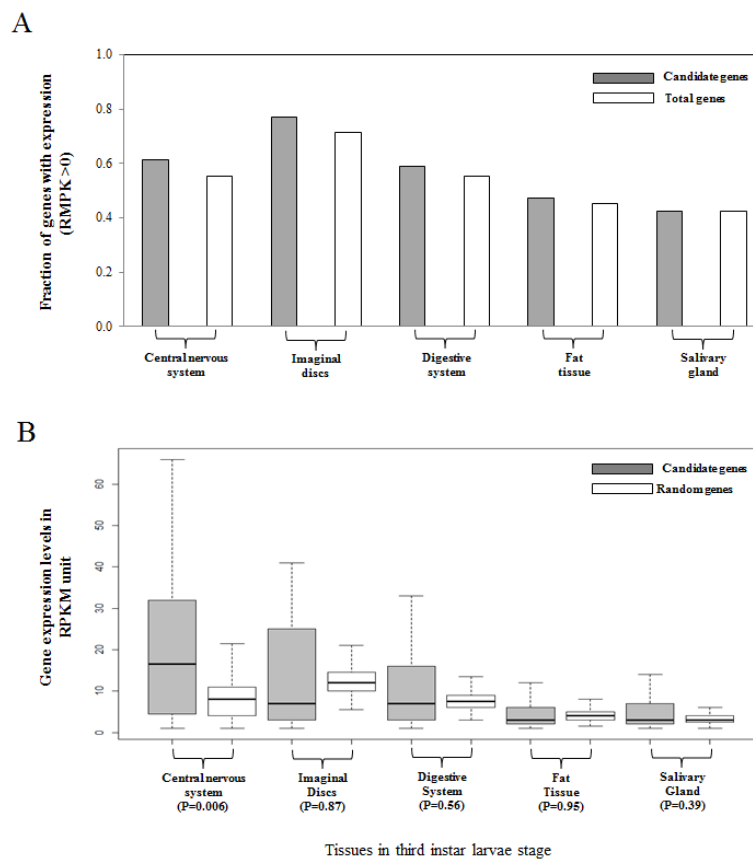


Figure 6: Tissue expression patterns of candidate genes in the third instar larvae stage. (A) Fraction of expressed genes (FPKM > 0) in different tissues of third instar larvae stage for both candidate genes, and total annotated protein-coding genes as control dataset. (B) Comparison of the gene expression levels in different tissues of third instar larvae stage for candidate genes and 1000 times randomly selected gene set, with the same sampling size of candidate gene set. The median expression value was taken to represent each time of random sampling. The statistical significances were computed with Wilcoxon rank sum test.

For 18 out of 81 (22%) genes in the 28 candidate regions, their genetic interactions have been documented in Flybase v6.19 (<http://www.flybase.org>) (Attrill et al., 2016). We used this information to construct a computationally predicted network of genetically interacting genes, allowing one intermediate gene (*i.e.*, a non-candidate gene connecting two candidate genes). This analysis revealed a network of 7 candidate genes from the GWA analyses and 17 computationally recruited intermediate genes (Figure 7). The probability that this network would have arisen when the same number of genes are randomly sampled is very low ($p < 2.2E-16$).

Given this network, we asked whether functional tests with genes from the network would confirm their involvement in the pupation height choice phenotype. Hence, we analysed the phenotypic effects of six computationally predicted genes (*Scrib*, *Pnt*, *Egfr*, *E2f1*, *p53* and *Ras85D*) in the above network (*Scrib* has been tested in the section of phenotype confirmations, see Figure 5), via direct comparisons of pupation height status between the co-isogenic progenitor stock and the respective gene disruption lines (Table 3) (strain details in Supplementary file 1D). Five of the six genes showed indeed a significant phenotypic effect on pupation height (P-value < 0.05), and the results were consistent for the disruption of different alleles for the same gene.

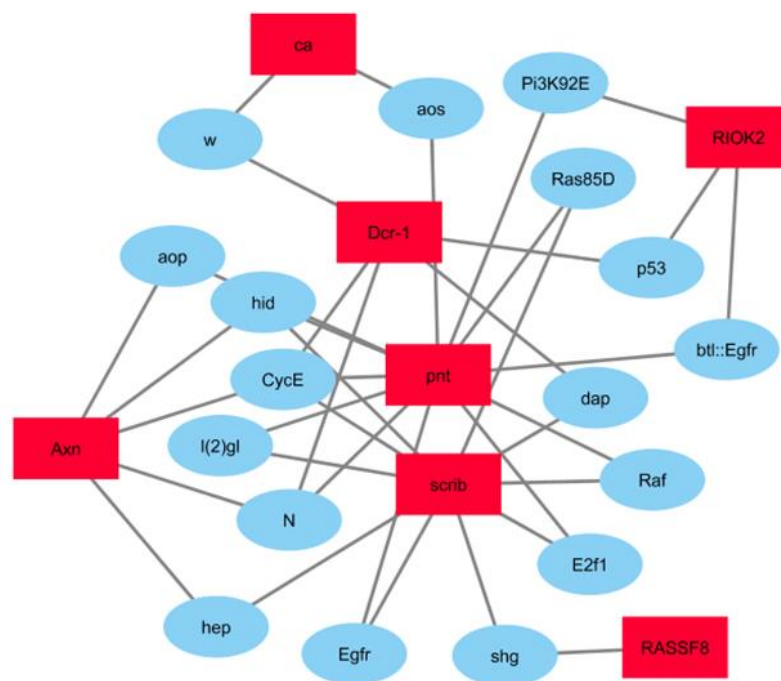


Figure 7: Gene interaction subnetwork connecting identified candidate genes. This gene interaction subnetwork that connects 7 candidate genes (coloured in red) through other 17 intermediate genes (coloured in blue).

362 **Table 3: Phenotypic effects of core network genes and randomly selected genes**

Dataset category	Tester gene	Pupation height GWA P-value	Expression in L3 tissues (RPKM)					Gene disruption region	Pupation height effect size (mm)	Pupae case length effect size (mm)	Tester (BDSC ID)	Progenitor (BDSC ID)
			CNS	Imaginal discs	Digestive system	Fat tissue	Salivary gland					
Network genes	<i>Scrib</i>	9.8E-06	15	19	14	2	3	CDS	-3.06 (SD:1.15)*	-0.01 (SD:0.05)	17791	6326
	<i>Pnt</i>	9.1E-06	7	6	10	2	0	Intron	0.80 (SD:4.38)	0.24 (SD:0.04)***	23004	5905
								5'UTR	-0.13 (SD:1.62)	0.02 (SD:0.02)*	12493	3605
	<i>Egfr</i>	8.0E-05	8	28	6	12	2	5'UTR	-14.28 (SD:3.77)***	-0.01 (SD:0.04)	20767	6599
	<i>E2f1</i>	2.1E-03	102	36	27	11	9	5'UTR	-13.96 (SD:2.04)***	0.18 (SD:0.04)***	22140	6599
								Intron	-17.82 (SD:2.78)***	0.02 (SD:0.02)**	17550	6599
Random genes	<i>P53</i>	3.5E-04	1	3	2	0	1	CDS	-18.67 (SD:1.78)***	0.08 (SD:0.03)***	20906	6599
	<i>Ras85D</i>	0.02	133	67	104	16	21	3'UTR	-15.87 (SD:1.90)***	0.11 (SD:0.03)***	15028	6599
	<i>Uif</i>	3.5E-03	9	43	5	1	0	CDS	10.46 (SD:2.77)***	0.04 (SD:0.02)***	61737	5905
	<i>Kek4</i>	2.7E-03	2	1	0	0	0	CDS	8.48 (SD:3.48)***	-0.11 (SD:0.04)***	26059	5905
	<i>Ddr</i>	4.3E-03	7	1	0	0	0	CDS	5.83 (SD:2.67)***	-0.08 (SD:0.03)***	26068	5905
	CG3711	7.7E-04	13	12	3	1	2	CDS	8.95 (SD:3.32)***	-0.04 (SD:0.02)***	23635	5905
	<i>Sgs1</i>	0.02	157	91	37	1	7557	CDS	9.38 (SD:4.28)***	-0.06 (SD:0.07)*	26359	5905
	ADD1	1.0E-03	24	29	5	2	1	CDS	6.71 (SD:2.75)***	0.02 (SD:0.07)	22992	5905
	CG9098	7.0E-03	20	2	4	0	0	CDS	-5.48 (SD:2.78)***	0.01 (SD:0.02)	24589	5905
	<i>Sgg</i>	4.6E-04	23	12	28	10	2	CDS	9.50 (SD:8.43)**	0.15 (SD:0.03)***	24680	5905
	CG5877	6.3E-04	8	24	6	1	3	CDS	6.91 (SD:3.24)***	0.10 (SD:0.10)**	61744	5905
	CG4281	8.6E-03	24	24	8	5	2	CDS	5.20 (SD:3.00)***	0.05 (SD:0.02)***	26331	5905
	CG3626	6.1E-04	8	9	6	5	2	CDS	4.87 (SD:2.32)***	0.11 (SD:0.03)***	29940	5905
	CG5177	8.8E-03	39	6	36	2	5	CDS	-3.08 (SD:1.73)***	0.12 (SD:0.05)***	29059	5905
	TTLL12	0.03	18	15	11	5	2	CDS	2.46 (SD:2.73)*	-0.03 (SD:0.03)*	23542	5905
	<i>Asph</i>	0.01	7	7	14	1	1	CDS	-3.66 (SD:3.74)*	-0.01 (SD:0.03)	24662	5905
	<i>Ptip</i>	2.0E-04	24	12	2	2	1	CDS	2.19 (SD:3.64)	0.10 (SD:0.04)***	27826	5905
	CG33639	0.02	6	0	0	0	0	CDS	3.98 (SD:4.73)*	0.11 (SD:0.06)***	29204	5905
	<i>Atg4a</i>	6.3E-03	9	8	16	8	3	CDS	-2.92 (SD:3.0)*	-0.05 (SD:0.07)	29214	5905
	CG9281	0.02	107	105	72	20	21	CDS	3.52 (SD:3.71)*	0.13 (SD:0.02)***	29230	5905
	<i>Ate1</i>	4.1E-03	17	37	14	5	4	CDS	2.07 (SD:2.71)*	0.08 (SD:0.11)*	29278	5905
	CG1674	0.13	5	1	1	0	1	CDS	-0.03 (SD:4.41)	0.07 (SD:0.06)**	26135	5905

- 363
- 364 **Note:**
- 365 1) The GWA P-value was defined as the lowest p-value from all the genetic variants within the gene and the 5kb up/down-stream of target gene;
- 366 2) The phenotypic effect size was defined as the deviation of pupation height/pupae case length of gene disruption stocks, compared with progenitor stocks;
- 367 3) Statistic significances: ***: P-value<0.001; **: P-value<0.01; *: P-value<0.05; otherwise P-value>0.05.

Phenotypic effects of randomly chosen genes

The omnigenic model (Boyle et al., 2017) predicts that most, if not all genes may modify the core network of a given quantitative trait, at least when they are expressed in the relevant developmental stage and organ(s). We have therefore set out to use our phenotyping pipeline to test this prediction. We selected 20 genes from the panel of *Drosophila* gene disruption stocks (Bellen et al., 2011) using the following criteria: 1) with expression in the CNS of third instar larvae stage (RPKM >0), 2) with transposon (Minos) disruption in the gene coding region, 3) derived from the same co-isogenic progenitor stock, and 4) homozygous disruption viable (strain details in Supplementary file 1E). The latter criterion biases against essential genes (approximately 30% are not homozygous viable), but otherwise the selection was essentially random. Intriguingly, we find again that the majority of genes (12 of 20) shows strongly significant effects ($p < 0.01$) and six additional ones marginally significant effects ($0.01 < p < 0.05$) on the pupation height choice phenotype (Table 3).

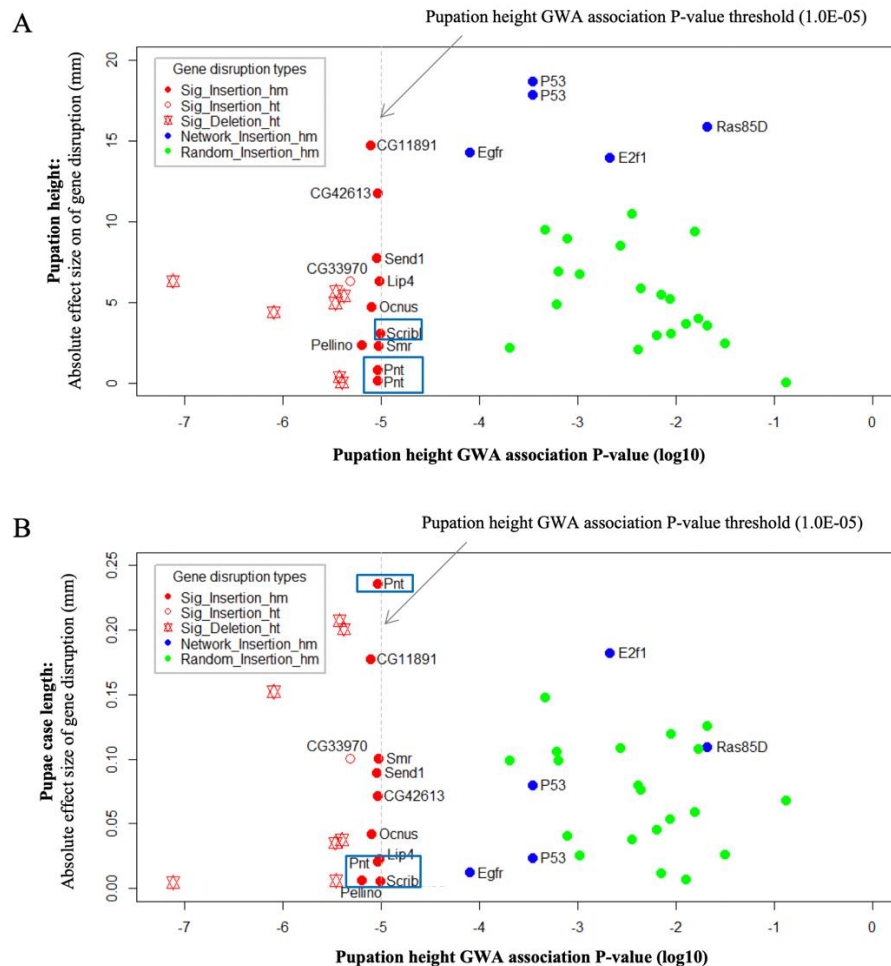


Figure 8: Comparison of pupation height GWA p-values and effect sizes on pupation height (A) and pupae case length (B) measured in gene disruption lines. Each dot represents one gene disruption line. The pupation height GWA P-value was defined as the lowest p-value from all the genetic variants within the gene and the 5kb up/down-stream of target gene. Sig_Insertion_hm/ht: homozygous/heterozygous transposon insertion lines for significant (GWA p-value <1E-05) associating genetic variants; Sig_Deletion_ht: heterozygous segmental deletion lines for significant associating genetic variants; Network_Insertion_hm: homozygous transposon insertion lines for genetic interaction network genes; Random_Insertion_hm: homozygous transposon insertion lines for random genes. The genes within blue rectangles are appearing as both significant GWA hits (P-value < 1.0E-05) and locating in the genetic interaction subnetwork.

Figure 8 - figure supplement 1: Comparison of pupation height GWA p-values and effect sizes of pupation height and pupae case length measured in gene homozygous disruption lines from transposon insertion mutagenesis.

Figure 8 compares the phenotypic effect sizes of the strains tested in this study with their respective pupation height GWAS p-values. It shows that the genes picked because of their GWA significance have not necessarily the largest phenotypic effects. However, the genes predicted from the network analysis (*i.e.*, *Egfr*, *E2f1*, *P53* and *Ras85D*), while not picked from GWA significance, show on average stronger effects on pupation height than other genes (Figure 8A, Wilcoxon rank sum test P-value: 2.5E-05). However, one could argue that these genes are general cell regulators that might affect many phenotypes. Hence, we checked also their effects on pupal case length that we measure with the same setup. We find that the effect sizes of these four genes on pupae case length are not particularly pronounced (Figure 8B) and are indistinguishable from average effect sizes of the randomly selected genes (Wilcoxon rank sum test P-value: 0.61). This supports the notion that the predicted network genes might indeed constitute the “core” genes of pupation height choice in *Drosophila melanogaster*.

However, one has to keep in mind that these strains may 1) have different genetic backgrounds, 2) have disruption in different regions, either coding regions or regulatory regions, 3) some of them only have the haplo-insufficient effects tested, and 4) some of them include deletions of multiple genes that required more complex crosses to detect their phenotypes (Supplementary file 1C). The first two factors seem to play only minor roles in the phenotype differences, given the observation that similar phenotypic effects can be found for the disruption of the same gene from different genetic background (Experimental result of *Pnt*, see Table 3), and different gene regions (Experimental result of *P53*, see Table 3). After removing gene disruption stocks with only haplo-insufficient effects tested and from segmental deletion, the genes predicted from the network analysis still show on average stronger phenotype effects on pupation height (Wilcoxon rank sum test P-value: 6.7E-05, see Figure 8 – figure supplement 1A), but not pupae case length (Wilcoxon rank sum test P-value: 0.45, see Figure 8 – figure supplement 1B).

Discussion

We have established a phenotyping pipeline for a behavioural trait in *Drosophila* that has allowed us to test predictions of the omnigenic model for quantitative traits (Boyle et al., 2017; Liu et al., 2019). Although it is debated whether the term is more useful than the long established terms “polygenic” and “infinitesimal” (Wray et al., 2018), the analysis by (Boyle et al., 2017) has certainly sparked new interest in this almost century-old question. Moreover, it implicitly includes the concept of core networks and their modifiers, which is a step forward compared to the previous definitions. But independent of the relative novelty, we are only now coming into a phase where predictions from these models can be directly tested. Most of the evidence has so far come from human studies, which are often focussed on disease questions and their associated special considerations and limitations (Wray et al., 2018). But for well-developed genetic model systems, such as *Drosophila*, one can do direct genetic experiments.

There is a fast increasing number of studies based on the DGRP panel that show high heritability of traits ($H^2 > 0.5$), but at the same time a polygenic architecture, even for cases where candidate genes have been predicted. This includes, for example, taste sensitivity to sugars (H^2 of 0.63) (Uchizono and Tanimura, 2017), sensitivity to lead toxicity (H^2 of 0.76) (Zhou et al., 2016), aggression (H^2 of 0.69) (Shorter et al., 2015), DDT resistance (H^2 of 0.8) (Schmidt et al., 2017), and adult foraging behaviour (h^2 of 0.52) (Lee et al., 2017). Hence, our finding and H^2 of 0.64 (h^2 of 0.46) for the pupation site choice and no major loci with genome wide significance is well within the framework of these other studies. Hence, it seems safe to assume that most studies on quantitative traits in this system will yield similar results.

But apart from stating that many genes of small effects are involved in a quantitative trait, the omnigenic concept makes two predictions. The first is that although very many loci may influence a trait, there would still be a set of core genes in a closely interacting network, the action of which is essential, while the other genes are modifiers. The second is that essentially all genes expressed in the relevant tissue and stage may be involved in the trait. We find that both of these predictions are fulfilled in our tests. We can identify a core network that makes predictions for other relevant genes in the

network (Figure 7 and 8). And we find that a large fraction of essentially randomly chosen genes have an effect on the phenotype (Figure 8 and Table 3).

Identification of a core network

Using the GWA *ad hoc* threshold of $p < 1.0E-05$, we were able to identify a set of 81 candidate genes within 28 associated genetic loci with significantly higher expression in CNS of L3 stage. Further, an interacting network was predicted among them, and the phenotypic effects on pupation height choice of five gene components from the network were experimentally confirmed. These include the well-studied gene *scribble* which encodes a scaffolding protein that is part of the conserved machinery regulating apicobasal polarity and organizes the synaptic architecture (Roche et al., 2002). This gene has also been reported to be associated with several other behavioural traits in *Drosophila melanogaster*, including olfactory behaviour (Ganguly et al., 2003), adult foraging (Lee et al., 2017) and sleep (Harbison et al., 2013). Another well-studied gene *Egfr*, which is the transmembrane tyrosine kinase receptor for signalling ligands in the TGF α family, was also found to function in neuronal development and behaviour traits in *Drosophila* (King et al., 2014; Potdar and Sheeba, 2013). *Ras85D* encodes a protein that acts downstream of several cell signals, most notably from Receptor Tyrosine Kinases (RTK), and has been reported to be involved in pupal size determination (Li et al., 2016). Another component of the network is *p53*, which is a general regulator of the cell cycle, but which has also been found to be involved in central nervous system development in *Drosophila* (Bauer et al., 2007) and behavioural traits, such as the entrainment of the circadian rhythm in mice (Hamada et al., 2014).

GWA versus genetics

The GWA p-value for the randomly chosen genes is below any threshold that one would normally consider using. Accordingly, none of them would have been identified as candidate genes. Most of them have been little studied so far and almost half of them have not even been named as yet (Table 3). Hence, they are indeed likely to act mostly as modifiers of other pathways. The reason why they have not shown up in the GWA could simply be that they do not include segregating variants of sufficient effect size in the population from which the DGRP was derived. In fact, one can expect that most genetic variants present in a natural *Drosophila* population are unlikely to represent gene disabling mutations. And the variants that are gene disabling should be rare, *i.e.*, should seldom occur as homozygotes. Hence, to test these genes as homozygous gene disruptions is rather unnatural. Still, it is an indication that the gene is involved in some form in the phenotype. But this is a general issue when comparing gene effects from a GWA analysis with those from classic genetic analyses. The former trace the effects of naturally occurring variants, the latter the ones of gene disruptions. These converge only for human genetic disease studies, but not for studies on natural genetic variation of quantitative traits. One has to keep this dichotomy of genetic views in mind when placing GWA results in the context of classic genetic results.

Conclusion

Our data confirm three major components of the omnigenic genetic architecture, namely that the trait under investigation is polygenic, that there is an underlying core network and that many randomly chosen genes can influence the trait. It should be possible to apply this test also to other phenotypes or genetic systems where the necessary stocks or experimental procedures are available. Evidently, if almost any random gene is involved in a given phenotype, why should one then do a GWA in the first place? Hence, it should be of special interest to study whether GWA p-values provide generally a guide to underlying core networks, as we have found here.

Materials and Methods

Drosophila strains

The list of strains of wildtype, DGRP inbred lines, transposon insertion /deficiency stocks, and their progenitor lines used in this study and their detailed information is provided in supplementary file 1. Flies were reared under standard culture conditions (cornmeal–molasses–agar medium, 24°C, 55–75% relative humidity, 12h light/dark cycle). A HOBO® data logger was placed in the incubator to monitor and record the environmental changes, *i.e.*, temperature, light and humidity, across all the experimental period.

Automated phenotyping of pupation height

A previously established automated pupal case length detection pipeline was adopted and modified for the automatic screening of pupation height measurements (Reeves and Tautz, 2017).

In brief, standard food was dispensed into 28.5 mm diameter and 95 mm height vials (Genesee Scientific), and the food height (defined as the distance from the surface of the food to the bottom of the vial) for each vial was manually measured and recorded. Once the food vials had fully cooled, 10.1 cm x 10.5 cm squares of overhead projector film (nobo, plain paper copier film, 33638237) were slid into each vial lining their entire vertical wall. Approximately 10 healthy female flies (15 for inbred stocks) and 5 healthy male flies were introduced into each vial, for which a custom printed semi-transparent label (GA International Inc.), including a unique barcode, was affixed to the outside of each vial. Adult flies were removed from the vials after 1-2 days and vials were kept in the same incubation condition (see above) for another 8-9 days to allow them to reach pupation stage. In general, by the 10th day after the parents were initially introduced, the majority of offspring in the vials were present as pupae attached to the transparent film. The film was gently moved out from each vial, the food from the lower part was scrapped away and any larvae or pupa at white puparium stage (P1) were removed. The film was then placed into a pre-made plastic frame, which holds the film flat for further photographing using bottom illumination in a light tight box. Batches of the resulting images were then introduced into the image analysis procedure.

An open-source public domain image analysis software called CellProfiler (v2.1.0) was applied for the simultaneous recognition of pupae and measurements of a variety of attributes, with a customized pipeline adopted and slightly modified from (Reeves and Tautz, 2017). In brief, any “primary object” with significant distinction from the background was first identified without restriction on their sizes (module: identify primary objects). By using the module called “Untangle Worms”, the above identified objects composing of multiple touching pupae were disentangled into distinct pupae. Furthermore, the resulting putative pupae were shrunk and re-propagated outwards for a more precise detection of the edges of each pupa based on boundary changes in pixel intensity (module “Identify secondary objects”). Finally, distinct attributes for the pupae were calculated and a specific confidence class was assigned for each pupa based on its size attribute. The digital outlines of pupae were overlaid onto a cropped version of the original image for easy visualization. Different from the pipeline described in (Reeves and Tautz, 2017), the methods used to distinguish clumped objects and to draw dividing lines between clumped objects were changed to be based on “shape”, as this increases the power of CellProfiler to resolve pupae in close proximity. A manual check on 40 randomly selected films showed that the CellProfiler pipeline can successfully identify 96% of true pupae (sensitivity), with an accuracy of 81% for identified putative pupae. To further improve the detection accuracy, an additional refinement criterion was defined based on the size attributes of “true” pupae from manual curation. Applying the new criteria, the accuracy for pupae detection was improved to around 99.85%, with only a tiny fraction (< 0.7%) of loss for true positive results.

In addition, a 1€ cent coin (16.25 mm diameter) was included in each image, for the control of camera coordinate changes and the conversion of measurements in pixels to millimetres. The pupation height for each pupal was calculated as the subtraction of the vial food height from the vertical coordinate measurement (CellProfiler parameter: Areashape_Y). Overlaid images and files with a variety of attribute measurements were imported into a FileMaker

database (v14, FileMaker Inc.). The quality filtering of pupae and related analysis were conducted with the tools implemented in the database.

Treatment of confounding factors

Pupal density in the vial is a biotic factor that could affect the pupation site selection preference of third instar larvae (Joshi and Mueller, 1993; Sokolowski and Hansell, 1983). Here, individually density was controlled through limiting the number of parents used per vial, and restricting the number of nights they remained before being cleared (see above). To further reduce the possible bias from low sampling effect, only vials with a pupal density of a minimum of 15 were considered as reliable, and a measurement for each stock should include at least 6 such reliable vial measurements. All of the tested stocks exhibited a uniformly positive relationship between individual density and pupation height estimate. The following equation was used to correct the influence of individual density in the vial on the mean estimate of pupation height:

$$\text{Pupation height corrected for individual density} = O + (D - M * S) \quad (1)$$

O: pupation height vial mean to be corrected

D: automated estimate of individual density in the vial to be corrected

M: average vial density across whole experiment (set as 70)

S: slope of regression of individual density against pupation height mean vial (set as 0.145)

To correct the influence from the change of incubator humidity and other cryptic abiotic factors, two wildtype stocks representing two extreme sides on pupation height (S-317 and S-314) were included and measured in each round of experiments for the phenotyping measurements of DGRP inbred stocks. The correction on incubation environment change was achieved with the following equation:

$$\text{Pupation height corrected for incubator environment change} = O - [(H - Hu) + (L - Lu)]/2 \quad (2)$$

O: pupation height of target DGRP stock from original measurement with correction of pupae density

H: pupation height measurement of high stock (S-314) for current round of experiment with correction of pupae density

Hu: average pupation height measurement of high stock (S-314) across all rounds of experiments with correction of pupae density

L: pupation height measurement of low stock (S-317) for current round of experiment with correction of pupae density

Lu: average pupation height measurement of low stock (S-317) across all rounds of experiments with correction of pupae density

Automatic measurement of pupal case length

The measurement of pupal case length followed the procedure described in (Reeves and Tautz, 2017). In brief, the pupal case length was defined as the length of the major axis of the ellipse that has the same normalized second central moments as the region of identified pupae, measured with the “Areashape_MajorAxisLength” index in CellProfiler. As the pupal case lengths are relatively robust to the pupal density in the vial and the minor change of incubator humidity, the measurement for pupal case length was not corrected for these factors.

Wolbachia infection, sex and maternal/paternal effect test

Two different approaches were exploited to test whether there is any effect on pupation site status from *Wolbachia* infection: 1) One indirect way applied here was to compare the difference of pupation height between *Wolbachia*-infected stocks and *Wolbachia*-uninfected stocks. 2) Three DGRP randomly chosen inbred lines with *Wolbachia* infection were used to create *Wolbachia*-free stocks through two generations of tetracycline treatment (by adding an appropriate volume of 100 mg/ml of tetracycline suspended in 99% ethanol to the surface of the solid prepared food) and then reared for at least another two generations with standard food to avoid any detrimental parental effects (Zeh et al., 2012). Meanwhile, half the flies from same three strains were also reared with standard food across the experiment as controls. Genomic DNA from the above 6 stocks was extracted individually using DNeasy blood and tissue kit (Qiagen), and the purity and concentration of the resulting DNA was measured with NanoDrop ND-1000 spectrophotometer (ThermoFisher). A diagnostic PCR to test for the presence of the *Wolbachia* *wsp* gene was done using the primers *wsp*81F (5'-tggtccaaaatgtgagaac-3') and *wsp*691r (5'-aaaattaaacgtactcca-3') (Richardson et al., 2012). The conditions for this diagnostic reaction were 35 cycles of 94°C for 15 seconds, 55°C for 30 seconds and 72°C for 1 minute. The expected PCR product length is around 630 bp. A standard (1%) agarose gel electrophoresis was used to test for the presence of the PCR product, with the broad range Quick DNA Marker (NEB #N0303) as loading ladder. Pupation height between the three *Wolbachia*-infected and the three *Wolbachia*-free lines were then measured and compared. In addition, the same procedure was applied to three randomly selected DGRP *Wolbachia*-uninfected lines to exclude the possibility that tetracycline treatment could have had an influence on pupation height.

One previously published dataset (Reeves and Tautz, 2017) consisting of pupation height and sex information on individuals was exploited to explore the presence of sexual dimorphism on pupation site status. In brief, 2,340 female pupae and 1,935 male pupae from 728 vials were randomly selected and their pupation site coordinate was measured and recorded. Deviation values from the corresponding vial average for all the sexed pupae were calculated, and the average deviation between two sexes were compared.

A reciprocal crossing approach was used to detect if any maternal, *e.g.*, genetic effect from mitochondria, or paternal effect for pupation site selection. Two pairs of high-low pupation height combinational DGRP inbred lines (DR_21 and DR_99; DR_73 and DR_81) were selected for this analysis. The pupation height of F1 offspring from two way of crossing, *i.e.*, virgin females from high stock crossing with males from low stock, and vice versa, were measured and compared with the phenotype of their parental stocks.

Estimates of heritability

The broad sense heritability (H^2) was estimated with the variance components of a linear model of the form: Phenotype = Population mean + Line effect + error (Schmidt et al., 2017). Total phenotypic variance was estimated as Genetic Variance + Environmental Variance, and the H^2 was thus estimated as G_v/G_v+E_v . This was implemented in IBM SPSS Statistics (version 22), with pupation height as the dependent variable and DGRP IL names as a random factor. Additionally, the measured number of pupae in each vial and the average humidity status during each round of experiment period were taken as covariates in the statistic model, to see whether the estimation was much influenced or not.

The narrow sense heritability was estimated as the proportion of variance in a phenotype explained by all available genetic variants used for mapping, an estimate that is often called “SNP heritability” (Wray et al., 2013). In practical, a genetic relationship matrix (GRM) between pairs of inbred strains from all the DGRP annotated genetic variants was built by using GEMMA (Version 0.96) (Zhou and Stephens, 2012), and then the narrow sense heritability (denoted as PVE) was calculated based on the above GRM with the univariate linear mixed model (Zhou and Stephens, 2012) implemented in GEMMA.

Principal component analysis (PCA) and genome-wide association analysis

The genetic variant information and major genomic inversion status were retrieved from DGRP freeze 2 (Huang et al., 2014). Genetic variants with missing values above 20% and minor allele frequency below 5% were excluded from further analysis, with which 1,903,028 genetic variants passing the stated criteria. To assess the possible influence of population structure on the pupation site selection, the PCA module from PLINK v1.90 (Purcell et al., 2007) was used to identify top principal components (PCs) from the filtered genetic variant data. The projection length of each strain on top 20 PCs was used to test the influence of cryptic population structures on pupation site selection.

The linear regression model implemented in PLINK (Purcell et al., 2007) was used to perform association analysis for the above filtered genetic variants. The R package “qqman” (Turner, 2014) was exploited for the visualization of GWA results in a Manhattan plot and qq-plots. Linear regression models used in this study include:

1) Pupation height ~ genotype

2) Pupation height ~ genotype + pupae case length

To define genome-wide significance threshold, we randomly assigned (1,000 times) phenotypes to individuals (thus preserving genetic structure), and performed mapping in PLINK, recording the lowest SNP association p - value for each permuted data set. The significance threshold (P-value <5E-8) was then defined as the 5th percentile of values for 1,000 permutations. As this stringent threshold returns no significant genetic variants, a more permissive significance threshold of p-value of 1E-5 was applied in practice. The associating genes for each genetic variant was predicted by SnpEff (Cingolani et al., 2012) with default parameters. In brief, all the protein-coding genes within 5 kb up/down-stream of target genetic variant were taken as its associating genes.

The genotypic linkage disequilibrium (LD) for each pair of significant genetic variants was tested by calculating the squared correlation estimator r^2 . Moreover, the r^2 values for each genetic variant and all other genetic variants were also computed. A significant genetic region (QTL) was defined by the position of the most distant downstream and upstream genetic variants showing a minimum r^2 of 0.8 to the significant genetic variants. Plink (Purcell et al., 2007) was used for all the r^2 calculations. All the associating genes as claimed above, together with the genes within the LD regions were considered as candidate genes for further analysis.

Functional validation experiments

Two types of gene disruption mutagenesis techniques were used to disrupt candidate genes: 1) transposon insertion in the candidate gene region (Bellen et al., 2011); 2) DNA segment deletion within which these candidate genes locate. The detailed information about the gene disruption stocks and their progenitors can be found in supplementary file 1. The transposon insertion introduces an early premature stop codon that can disrupt the protein synthesis of candidate gene or disrupts the regulatory elements that could alter the expression of the candidate gene, and the deficiency mutation is the stock with approximately 10kb DNA segment deletion, within which the candidate gene locates. Based on the gene disruption type and selection marker on the balancer chromosome, the functional validation experiments were conducted as follows:

1) Transposon insertion lines: homozygous insertion complete-viable

The pupation height status of the transposon insertion lines and their corresponding progenitor lines are directly measured and compared.

2) Transposon insertion lines: homozygous insertion semi-lethal (or semi-viable)

Only virgin flies with homozygous insertion from these transposon insertion strains were selected for experiment validation. The pupation height status of the transposon insertion lines and their corresponding progenitor lines are then measured and compared.

3) Homozygous deficiency complete-lethal: with detectable marker (*Tubby*) at pupae stage

Four out of seven deficiency stocks are segregating balancer chromosomes with *Tb* selection marker (short rounded pupal), due to the complete lethality of homozygous large DNA segment deletion. The pupation site choices of the background stock (BG line) and F1 generation of the crossing of each segment deletion stock (virgin females) and its BG stock (males) were measured with the phenotyping pipeline aforementioned. The pupation height statuses of hemi-deletion individuals without *Tb* markers (no presence of balancer chromosome) were compared with those from BG stocks. The absence of *Tb* marker for individual pupal was determined by its pupae case length (> 73 pixels for *Areashape_major_len* from the output of Cellprofiler), on the basis of the apparent distinction between individual pupae with and without *Tb* markers. Moreover, manual check was done to further separate ambiguous individuals.

4) Homozygous insertion/deficiency complete-lethal: without detectable marker at pupae stage

One transposon insertion line and three deficiency lines are segregating balancer chromosomes with no detectable marker at pupal stage (*curly wing* or *stubble*), due to the complete lethality of homozygous large DNA segment deletion. Virgin female individuals from these insertion or deficiency stocks were crossed with male individuals from BG lines to generate F1 generation. Virgin female individuals without screening markers at adult stage from the F1 generation were selected and backcrossed with males from the BG lines. The pupation height status of the F2 generation were measured and compared with that of their progenitor stocks. It is worthwhile to note that the detected significances of the phenotyping effect of candidate genes from this approach are likely to be underestimated, as only half of the individuals in the experimental group are expected to contain the gene semi-deletion.

Expression and genetic interaction network analysis

The gene expression profiling data from Drosophila modENCODE project (Brown et al., 2014) were used for expression analysis. These were generated by measuring the genome-wide gene expression for 5 tissues in third instar larvae stages, including central nervous system (CNS), digestive system, fat, image disc and saliva glands. The expression level for each gene within each tissue was measured in units of RPKM. The fraction of genes with expression (RPKM >0) in candidate genes were compared with that in total annotated protein-coding genes. Moreover, the average gene expression levels for expressed candidate genes were also compared with those from (1000 times) randomly selected genes with the same dataset size.

The genetic interaction database was directly downloaded from Flybase V6.19 (Attrill et al., 2016). A network for whose edges were either a direct connection between candidate genes or bridged by only one gene not among the candidate gene list was extracted. The significance of the size of the largest cluster among the subnetworks by a randomization test in which we randomly extracted subnetworks for 1000 times with the same number of input genes. The *p*-value was determined by dividing the number of instances where the size of the largest cluster exceeds the observed largest size by the total number of randomizations (Zhou et al., 2016).

Moreover, phenotypic effects of six genes (*Scrib*, *Pnt*, *Egfr*, *E2f1*, *p53* and *Ras85D*) in the above network were further checked, via direct comparisons of pupation height status between the co-isogenic progenitor stock and transposon disruption of each target gene (supplementary file 1D). In case there is no disruption line in the gene coding region, the ones with transposon disruption in gene regulatory regions (e.g., Intron or UTR) were selected for

experimental variation. The phenotyping test experiments were conducted with the same procedure as above functional validation experiment.

Phenotypic effect test on random stocks

20 gene disruption stocks from the panel of *Drosophila* gene disruption project (Bellen et al., 2011) were selected using the following criteria: 1) with expression in the CNS of third instar larvae stage (RPKM >0), 2) with disruption in the gene coding region by the same type of transposon (Minos), 3) derived from the same co-isogenic progenitor stock, and 4) homozygous disruption viable. The phenotyping test experiments were conducted with the same procedure as above functional validation experiment. The GWA association p-value was taken as the lowest p-values from all the genetic variants within the gene and the 5kb up/down-stream of target gene.

Data availability

All the *Drosophila melanogaster* strains used in this study are public available through either Bloomington *Drosophila* Stock centre (<https://bdsc.indiana.edu/>) or EHIME *Drosophila* stock centre (<https://kyotofly.kit.jp/cgi-bin/ehime/index.cgi>). The detailed information about the wildtype, DGRP inbred lines and gene disruption stocks, is provided in Supplementary file 1. The primers used for *Wolbachia* infection detection are listed in the above text of this section.

Acknowledgements

We are grateful to Wen Huang for help on *Drosophila* Genetic Reference Panel (DGRP) stocks. We appreciate Tautz's lab members for helpful discussions and suggestions. We thank Anita Moeller and Elke Blohm Sievers for their excellent technical help and advice with conducting this experiment. This work was supported by institutional funding through the Max-Planck Society.

Competing interests

DT: Senior editor, eLife. The other authors declare that no competing interests exist.

Supporting information

Supplementary file 1: Information for the fly stocks used in this study.

References

- Attrill H, Falls K, Goodman JL, Millburn GH, Antonazzo G, Rey AJ, Marygold SJ. 2016. Flybase: Establishing a gene group resource for *Drosophila melanogaster*. *Nucleic Acids Res.* doi:10.1093/nar/gkv1046
- Bauer JH, Chang C, Morris SNS, Hozier S, Andersen S, Waitzman JS, Helfand SL. 2007. Expression of dominant-negative Dmp53 in the adult fly brain inhibits insulin signaling. *Proc Natl Acad Sci.* doi:10.1073/pnas.0706121104

- 717 Bellen HJ, Levis RW, He Y, Carlson JW, Evans-Holm M, Bae E, Kim J, Metaxakis A, Savakis C, Schulze KL,
718 Hoskins RA, Spradling AC. 2011. The *Drosophila* gene disruption project: Progress using transposons with
719 distinctive site specificities. *Genetics* **188**:731–743. doi:10.1534/genetics.111.126995
- 720 Boyle EA, Li YI, Pritchard JK. 2017. An Expanded View of Complex Traits: From Polygenic to Omnigenic. *Cell*.
721 doi:10.1016/j.cell.2017.05.038
- 722 Brown JB, Boley N, Eisman R, May GE, Stoiber MH, Duff MO, Booth BW, Wen J, Park S, Suzuki AM, Wan KH,
723 Yu C, Zhang D, Carlson JW, Cherbas L, Eads BD, Miller D, Mockaitis K, Roberts J, Davis CA, Frise E,
724 Hammonds AS, Olson S, Shenker S, Sturgill D, Samsonova AA, Weiszmann R, Robinson G, Hernandez J,
725 Andrews J, Bickel PJ, Carninci P, Cherbas P, Gingeras TR, Hoskins RA, Kaufman TC, Lai EC, Oliver B,
726 Perrimon N, Graveley BR, Celniker SE. 2014. Diversity and dynamics of the *Drosophila* transcriptome. *Nature*
727 **512**:393–399. doi:10.1038/nature12962
- 728 Carpenter AE, Jones TR, Lamprecht MR, Clarke C, Kang IH, Friman O, Guertin DA, Chang JH, Lindquist RA,
729 Moffat J, Golland P, Sabatini DM. 2006. CellProfiler: Image analysis software for identifying and quantifying
730 cell phenotypes. *Genome Biol* **7**. doi:10.1186/gb-2006-7-10-r100
- 731 Casares P, Carracedo M, García-Florez L. 1997. Analysis of larval behaviours underlying the pupation height
732 phenotype in *Drosophila simulans* and *D. melanogaster*. *Genet Sel Evol* **29**:589. doi:10.1186/1297-9686-29-5-
733 589
- 734 Casares P, Carracedo MC. 1987. Pupation height in *Drosophila*: Sex differences and influence of larval
735 developmental time. *Behav Genet* **17**:523–535. doi:10.1007/BF01073119
- 736 Casares P, Carracedo MC. 1986. On selecting for pupation height in *Drosophila simulans*. *Experientia* **42**:1289–1291.
737 doi:10.1007/BF01946427
- 738 Cingolani P, Platts A, Wang LL, Coon M, Nguyen T, Wang L, Land SJ, Lu X, Ruden DM. 2012. A program for
739 annotating and predicting the effects of single nucleotide polymorphisms, SnpEff: SNPs in the genome of
740 *Drosophila melanogaster* strain w1118; iso-2; iso-3. *Fly (Austin)*. doi:10.4161/fly.19695
- 741 Dembeck LM, Huang W, Magwire MM, Lawrence F, Lyman RF, Mackay TFC. 2015. Genetic Architecture of
742 Abdominal Pigmentation in *Drosophila melanogaster*. *PLoS Genet* **11**. doi:10.1371/journal.pgen.1005163
- 743 Durham MF, Magwire MM, Stone EA, Leips J. 2014. Genome-wide analysis in *Drosophila* reveals age-specific
744 effects of SNPs on fitness traits. *Nat Commun* **5**. doi:10.1038/ncomms5338
- 745 Erezylmaz DF, Stern DL. 2013. Pupariation site preference within and between *drosophila* sibling species. *Evolution*
746 (*N Y*) **67**:2714–2727. doi:10.1111/evo.12146
- 747 Ganguly I, Mackay TFC, Anholt RRH. 2003. Scribble is essential for olfactory behavior in *Drosophila melanogaster*.
748 *Genetics*.
- 749 Garcia-Flores L, Casares P, Carracedo C. 1989. Selection for pupation height in *Drosophila melanogaster*. *Genetica*
750 **155**–160.
- 751 Hamada T, Niki T, Ishida N. 2014. Role of p53 in the entrainment of mammalian circadian behavior rhythms. *Genes*
752 *to Cells*. doi:10.1111/gtc.12144
- 753 Harbison ST, McCoy LJ, Mackay TFC. 2013. Genome-wide association study of sleep in *Drosophila melanogaster*.
754 *BMC Genomics*. doi:10.1186/1471-2164-14-281
- 755 Harini BP. 2013. Interspecies Variation in Pupation Site Preference on Exposure to Different Anti Epileptic Drugs -
756 A Study in Few Species of *Drosophila*. *Int J Sci Res ISSN (Online Index Copernicus Value Impact Factor*
757 **14611**:2319–7064.
- 758 Hodge S, Caslaw P. 1998. The effect of resource pH on pupation height in *Drosophila* (Diptera : *Drosophilidae*). *J*
759 *Insect Behav* **11**:47–57.

- 760 Hoffmann AA, Rieseberg LH. 2008. Revisiting the Impact of Inversions in Evolution: From Population Genetic
761 Markers to Drivers of Adaptive Shifts and Speciation? *Annu Rev Ecol Evol Syst* **39**:21–42.
762 doi:10.1146/annurev.ecolsys.39.110707.173532
- 763 Huang W, Massouras A, Inoue Y, Peiffer J, Ràmia M, Tarone AM, Turlapati L, Zichner T, Zhu D, Lyman RF,
764 Magwire MM, Blankenburg K, Carbone MA, Chang K, Ellis LL, Fernandez S, Han Y, Highnam G, Hjelman
765 CE, Jack JR, Javaid M, Jayaseelan J, Kalra D, Lee S, Lewis L, Munidasa M, Ongeri F, Patel S, Perales L,
766 Perez A, Pu LL, Rollmann SM, Ruth R, Saada N, Warner C, Williams A, Wu YQ, Yamamoto A, Zhang Y,
767 Zhu Y, Anholt RRH, Korbel JO, Mittelman D, Muzny DM, Gibbs RA, Barbadilla A, Johnston JS, Stone EA,
768 Richards S, Deplancke B, Mackay TFC. 2014. Natural variation in genome architecture among 205 *Drosophila*
769 *melanogaster* Genetic Reference Panel lines. *Genome Res* **24**:1193–1208. doi:10.1101/gr.171546.113
- 770 Jones MDR, Reiter P. 1975. Entrainment of the pupation and adult activity rhythms during development in the
771 mosquito *Anopheles gambiae*. *Nature* **254**:242–244. doi:10.1038/254242a0
- 772 Joshi A, Mueller L. 1993. Directional and Stabilizing Density-Dependent Natural Selection for Pupation Height in
773 *Drosophila melanogaster*. *Evolution (N Y)* **47**:176–184.
- 774 King IFG, Eddison M, Kaun KR, Heberlein U. 2014. EGFR and FGFR pathways have distinct roles in *drosophila*
775 mushroom body development and ethanol-induced behavior. *PLoS One*. doi:10.1371/journal.pone.0087714
- 776 Lee YCG, Yang Q, Chi W, Turkson SA, Du WA, Kemkemmer C, Zeng ZB, Long M, Zhuang X. 2017. Genetic
777 architecture of natural variation underlying adult foraging behavior that is essential for survival of *Drosophila*
778 *melanogaster*. *Genome Biol Evol* **9**:1357–1369. doi:10.1093/gbe/evx089
- 779 Li Y, Li S, Jin P, Chen L, Ma F. 2016. miR-11 regulates pupal size of *Drosophila melanogaster* via directly targeting
780 Ras85D. *Am J Physiol Physiol*. doi:10.1152/ajpcell.00190.2016
- 781 Liu X, Li YI, Pritchard JK. 2019. Trans Effects on Gene Expression Can Drive Omnigenic Inheritance. *Cell*
782 **177**:1022–1034.e6. doi:10.1016/j.cell.2019.04.014
- 783 Mackay TFC, Huang W. 2018. Charting the genotype–phenotype map: lessons from the *Drosophila melanogaster*
784 Genetic Reference Panel. *Wiley Interdiscip Rev Dev Biol*. doi:10.1002/wdev.289
- 785 MacKay TFC, Richards S, Stone EA, Barbadilla A, Ayroles JF, Zhu D, Casillas S, Han Y, Magwire MM, Cridland
786 JM, Richardson MF, Anholt RRH, Barrón M, Bess C, Blankenburg KP, Carbone MA, Castellano D, Chaboub
787 L, Duncan L, Harris Z, Javaid M, Jayaseelan JC, Jhangiani SN, Jordan KW, Lara F, Lawrence F, Lee SL,
788 Librado P, Linheiro RS, Lyman RF, MacKey AJ, Munidasa M, Muzny DM, Nazareth L, Newsham I, Perales L,
789 Pu LL, Qu C, Ràmia M, Reid JG, Rollmann SM, Rozas J, Saada N, Turlapati L, Worley KC, Wu YQ,
790 Yamamoto A, Zhu Y, Bergman CM, Thornton KR, Mittelman D, Gibbs RA. 2012. The *Drosophila*
791 *melanogaster* Genetic Reference Panel. *Nature* **482**:173–178. doi:10.1038/nature10811
- 792 Markow TA. 1981. Light-dependent pupation site preferences in *Drosophila*: Behavior of adult visual mutants.
793 *Behav Neural Biol* **31**:348–353. doi:10.1016/S0163-1047(81)91409-6
- 794 Markow TA. 1979. A survey of intra- and interspecific variation for pupation height in *Drosophila*. *Behav Genet*
795 **9**:209–217. doi:10.1007/BF01071301
- 796 Pallares LF, Harr B, Turner LM, Tautz D. 2014. Use of a natural hybrid zone for genomewide association mapping
797 of craniofacial traits in the house mouse. *Mol Ecol* **23**:5756–5770. doi:10.1111/mec.12968
- 798 Potdar S, Sheeba V. 2013. Lessons from sleeping flies: Insights from *Drosophila melanogaster* on the Neuronal
799 circuitry and importance of sleep. *J Neurogenet*. doi:10.3109/01677063.2013.791692
- 800 Price AL, Zaitlen NA, Reich D, Patterson N. 2010. New approaches to population stratification in genome-wide
801 association studies. *Nat Rev Genet*. doi:10.1038/nrg2813
- 802 Price GM. 1970. Pupation Inhibiting Factor in the Larva of the Blowfly *Calliphora erythrocephala*. *Nature* **228**:876–
803 877. doi:10.1038/228876a0

804 Purcell S, Neale B, Todd-Brown K, Thomas L, Ferreira MAR, Bender D, Maller J, Sklar P, de Bakker PIW, Daly MJ,
805 Sham PC. 2007. PLINK: A Tool Set for Whole-Genome Association and Population-Based Linkage Analyses.
806 *Am J Hum Genet* **81**:559–575. doi:10.1086/519795

807 Reeves RG, Tautz D. 2017. Automated Phenotyping Indicates Pupal Size in *Drosophila* Is a Highly Heritable Trait
808 with an Apparent Polygenic Basis. *G3 (Bethesda)* **7**:1277–1286. doi:10.1534/g3.117.039883

809 Richardson MF, Weinert LA, Welch JJ, Linheiro RS, Magwire MM, Jiggins FM, Bergman CM. 2012. Population
810 Genomics of the Wolbachia Endosymbiont in *Drosophila melanogaster*. *PLoS Genet* **8**.
811 doi:10.1371/journal.pgen.1003129

812 Riedl CAL, Riedl M, Mackay TFC, Sokolowski MB. 2007. Genetic and behavioral analysis of natural variation in
813 *Drosophila melanogaster* pupation position. *Fly (Austin)* **1**:23–32. doi:3830 [pii]

814 Roche JP, Packard MC, Moeckel-Cole S, Budnik V. 2002. Regulation of synaptic plasticity and synaptic vesicle
815 dynamics by the PDZ protein Scribble. *J Neurosci* **22**:6471–9. doi:20026646

816 Rodriguez L, Sokolowski MB, Shore JS. 1992. Habitat selection by *Drosophila melanogaster* larvae. *J Evol Biol*
817 **70**:61–70. doi:10.1046/j.1420-9101.1992.5010061.x

818 Rohde PD, Gaertner B, Ward K, Sørensen P, Mackay TFC. 2017. Genomic analysis of genotype-by-social
819 environment interaction for *Drosophila melanogaster* aggressive behavior. *Genetics* **206**:1969–1984.
820 doi:10.1534/genetics.117.200642

821 Schmidt JM, Battlay P, Gledhill-Smith RS, Good RT, Lumb C, Fournier-Level A, Robin C. 2017. Insights into DDT
822 resistance from the *Drosophila melanogaster* genetic reference panel. *Genetics* **207**:1181–1193.
823 doi:10.1534/genetics.117.300310

824 Schnebel EM, Grossfield J. 1992. Temperature effects on pupation-height response in four *Drosophila* species group
825 triads. *J Insect Physiol* **38**:121–132.

826 Schnebel EM, Grossfield J. 1986. The influence of light on pupation height in *Drosophila*. *Behav Genet* **16**:407–413.
827 doi:10.1007/BF01071320

828 Sharon J. Bauer and MBS. 1985. A genetic analysis of path length and pupation height in a natural population of
829 *Drosophila melanogaster*. *Can J Genet Cytol* **27**:334–340. doi:10.1139/g85-050

830 Shorter J, Couch C, Huang W, Carbone MA, Peiffer J, Anholt RRRH, Mackay TFC. 2015. Genetic architecture of
831 natural variation in *Drosophila melanogaster* aggressive behavior. *Proc Natl Acad Sci U S A* **112**:E3555–63.
832 doi:10.1073/pnas.1510104112

833 Singh BN, Pandey MB. 1993. Selection for High and Low Pupation Height in *Drosophila ananassae*. *Behav Genet*
834 **23**:239–243.

835 Sokal RR, Ehrlich PR, Hunter PE, Schlager G. 1960. Some factors affecting pupation site of *Drosophila*. *Ann Ent*
836 *Soc Amer* **53**:174–182. doi:10.1093/aesa/53.2.174

837 Sokolowski MB. 1985. Genetics and ecology of *Drosophila melanogaster* larval foraging and pupation behaviour. *J*
838 *Insect Physiol* **31**:857–864. doi:10.1016/0022-1910(85)90103-9

839 Sokolowski MB, Bauer SJ. 1989. Genetic analyses of pupation distance in *Drosophila melanogaster*. *Heredity (Edinb)*
840 **62**:177–183. doi:10.1038/hdy.1989.26

841 Sokolowski MB, Hansell RIC. 1983. Elucidating the behavioral phenotype of *Drosophila melanogaster* larvae:
842 Correlations between larval foraging strategies and pupation height. *Behav Genet* **13**:267–280.
843 doi:10.1007/BF01071872

844 Turner SD. 2014. qqman: an R package for visualizing GWAS results using Q-Q and manhattan plots, bioRxiv.
845 doi:10.1101/005165

- 846 Uchizono S, Tanimura T. 2017. Genetic variation in taste sensitivity to sugars in drosophila melanogaster. *Chem*
847 *Senses* **42**:287–294. doi:10.1093/chemse/bjw165
- 848 Vandal NB, N.Shivanna, A.Modagi S. 2012. Larval pupation site preference in Different species of Drosophila:
849 Larval pupation in Drosophila. Lambert Academic Publishing.
- 850 Vandal NB, Siddalingamurthy GS, Shivanna N. 2008. Larval pupation site preference on fruit in different species of
851 Drosophila. *Entomol Res* **38**:188–194. doi:10.1111/j.1748-5967.2008.00163.x
- 852 Welbergen P, Sokolowski MB. 1994. Development time and pupation behavior in the Drosophila melanogaster
853 subgroup (Diptera: Drosophilidae). *J Insect Behav* **7**:263–277. doi:10.1007/BF01989734
- 854 Wood AR, Esko T, Yang J, Vedantam S, Pers TH, Gustafsson S, Chu AY, Estrada K, Luan J, Kutalik Z, Amin N,
855 Buchkovich ML, Croteau-Chonka DC, Day FR, Duan Y, Fall T, Fehrmann R, Ferreira T, Jackson AU,
856 Karjalainen J, Lo KS, Locke AE, Mägi R, Mihailov E, Porcu E, Randall JC, Scherag A, Vinkhuyzen AAE,
857 Westra HJ, Winkler TW, Workalemahu T, Zhao JH, Absher D, Albrecht E, Anderson D, Baron J, Beekman M,
858 Demirkan A, Ehret GB, Feenstra B, Feitosa MF, Fischer K, Fraser RM, Goel A, Gong J, Justice AE, Kanoni S,
859 Kleber ME, Kristiansson K, Lim U, Lotay V, Lui JC, Mangino M, Leach IM, Medina-Gomez C, Nalls MA,
860 Nyholt DR, Palmer CD, Pasko D, Pechlivanis S, Prokopenko I, Ried JS, Ripke S, Shungin D, Stancáková A,
861 Strawbridge RJ, Sung YJ, Tanaka T, Teumer A, Trompet S, Van Der Laan SW, Van Setten J, Van Vliet-
862 Ostaptchouk J V., Wang Z, Yengo L, Zhang W, Afzal U, Ärnlöv J, Arscott GM, Bandinelli S, Barrett A, Bellis
863 C, Bennett AJ, Berne C, Blüher M, Bolton JL, Böttcher Y, Boyd HA, Bruinenberg M, Buckley BM, Buyske S,
864 Caspersen IH, Chines PS, Clarke R, Claudi-Boehm S, Cooper M, Daw EW, De Jong PA, Deelen J, Delgado G,
865 Denny JC, Dhonukshe-Rutten R, Dimitriou M, Doney ASF, Dörr M, Eklund N, Eury E, Folkersen L, Garcia
866 ME, Geller F, Giedraitis V, Go AS, Grallert H, Grammer TB, Gräßler J, Grönberg H, De Groot LCPGM,
867 Groves CJ, Haessler J, Hall P, Haller T, Hallmans G, Hannemann A, Hartman CA, Hassinen M, Hayward C,
868 Heard-Costa NL, Helmer Q, Hemani G, Henders AK, Hillege HL, Hlatky MA, Hoffmann W, Hoffmann P,
869 Holmen O, Houwing-Duistermaat JJ, Illig T, Isaacs A, James AL, Jeff J, Johansen B, Johansson Å, Jolley J,
870 Juliusdottir T, Junttila J, Kho AN, Kinnunen L, Klopp N, Kocher T, Kratzer W, Lichtner P, Lind L, Lindström
871 J, Lobbens S, Lorentzon M, Lu Y, Lyssenko V, Magnusson PKE, Mahajan A, Maillard M, McArdle WL,
872 McKenzie CA, McLachlan S, McLaren PJ, Menni C, Merger S, Milani L, Moayyeri A, Monda KL, Morken
873 MA, Müller G, Müller-Nurasyid M, Musk AW, Narisu N, Nauck M, Nolte IM, Nöthen MM, Oozageer L, Pilz
874 S, Rayner NW, Renstrom F, Robertson NR, Rose LM, Roussel R, Sanna S, Scharnagl H, Scholtens S,
875 Schumacher FR, Schunkert H, Scott RA, Sehmi J, Seufferlein T, Shi J, Silventoinen K, Smit JH, Smith AV,
876 Smolonska J, Stanton A V., Stirrups K, Stott DJ, Stringham HM, Sundström J, Swertz MA, Syvänen AC, Tayo
877 BO, Thorleifsson G, Tyrer JP, Van Dijk S, Van Schoor NM, Van Der Velde N, Van Heemst D, Van Oort FVA,
878 Vermeulen SH, Verweij N, Vonk JM, Waite LL, Waldenberger M, Wennauer R, Wilkens LR, Willenborg C,
879 Wilsgaard T, Wojczynski MK, Wong A, Wright AF, Zhang Q, Arveiler D, Bakker SJL, Beilby J, Bergman RN,
880 Bergmann S, Biffar R, Blangero J, Boomsma DI, Bornstein SR, Bovet P, Brambilla P, Brown MJ, Campbell H,
881 Caulfield MJ, Chakravarti A, Collins R, Collins FS, Crawford DC, Cupples LA, Danesh J, De Faire U, Den
882 Ruijter HM, Erbel R, Erdmann J, Eriksson JG, Farrall M, Ferrannini E, Ferrières J, Ford I, Forouhi NG,
883 Forrester T, Gansevoort RT, Gejman P V., Gieger C, Golay A, Gottesman O, Gudnason V, Gyllenstein U, Haas
884 DW, Hall AS, Harris TB, Hattersley AT, Heath AC, Hengstenberg C, Hicks AA, Hindorff LA, Hingorani AD,
885 Hofman A, Hovingh GK, Humphries SE, Hunt SC, Hyponen E, Jacobs KB, Jarvelin MR, Jousilahti P, Jula
886 AM, Kaprio J, Kastelein JJP, Kayser M, Kee F, Keinanen-Kiukaanniemi SM, Kiemeny LA, Kooner JS,
887 Kooperberg C, Koskinen S, Kovacs P, Kraja AT, Kumari M, Kuusisto J, Lakka TA, Langenberg C, Le
888 Marchand L, Lehtimäki T, Lupoli S, Madden PAF, Männistö S, Manunta P, Marette A, Matise TC, McKnight
889 B, Meitinger T, Moll FL, Montgomery GW, Morris AD, Morris AP, Murray JC, Nelis M, Ohlsson C,
890 Oldehinkel AJ, Ong KK, Ouwehand WH, Pasterkamp G, Peters A, Pramstaller PP, Price JF, Qi L, Raitakari
891 OT, Rankinen T, Rao DC, Rice TK, Ritchie M, Rudan I, Salomaa V, Samani NJ, Saramies J, Sarzynski MA,
892 Schwarz PEH, Sebert S, Sever P, Shuldiner AR, Sinisalo J, Steinthorsdottir V, Stolk RP, Tardif JC, Tönjes A,
893 Tremblay A, Tremoli E, Virtamo J, Vohl MC, Amouyel P, Asselbergs FW, Assimes TL, Bochud M, Boehm
894 BO, Boerwinkle E, Bottinger EP, Bouchard C, Cauchi S, Chambers JC, Chanock SJ, Cooper RS, De Bakker
895 PIW, Dedoussis G, Ferrucci L, Franks PW, Froguel P, Groop LC, Haiman CA, Hamsten A, Hayes MG, Hui J,
896 Hunter DJ, Hveem K, Jukema JW, Kaplan RC, Kivimäki M, Kuh D, Laakso M, Liu Y, Martin NG, März W,
897 Melbye M, Moebus S, Munroe PB, Njølstad I, Oostra BA, Palmer CNA, Pedersen NL, Perola M, Pérusse L,
898 Peters U, Powell JE, Power C, Quertermous T, Rauramaa R, Reinmaa E, Ridker PM, Rivadeneira F, Rotter JJ,

899 Saaristo TE, Saleheen D, Schlessinger D, Slagboom PE, Snieder H, Spector TD, Strauch K, Stumvoll M,
900 Tuomilehto J, Uusitupa M, Van Der Harst P, Völzke H, Walker M, Wareham NJ, Watkins H, Wichmann HE,
901 Wilson JF, Zanen P, Deloukas P, Heid IM, Lindgren CM, Mohlke KL, Speliotes EK, Thorsteinsdottir U,
902 Barroso I, Fox CS, North KE, Strachan DP, Beckmann JS, Berndt SI, Boehnke M, Borecki IB, McCarthy MI,
903 Metspalu A, Stefansson K, Uitterlinden AG, Van Duijn CM, Franke L, Willer CJ, Price AL, Lettre G, Loos
904 RJF, Weedon MN, Ingelsson E, O'Connell JR, Abecasis GR, Chasman DI, Goddard ME, Visscher PM,
905 Hirschhorn JN, Frayling TM. 2014. Defining the role of common variation in the genomic and biological
906 architecture of adult human height. *Nat Genet.* doi:10.1038/ng.3097

907 Wray NR, Wijmenga C, Sullivan PF, Yang J, Visscher PM. 2018. Common Disease Is More Complex Than Implied
908 by the Core Gene Omnigenic Model. *Cell.* doi:10.1016/j.cell.2018.05.051

909 Wray NR, Yang J, Hayes BJ, Price AL, Goddard ME, Visscher PM. 2013. Pitfalls of predicting complex traits from
910 SNPs. *Nat Rev Genet.* doi:10.1038/nrg3457

911 Xue A, Wang H, Zhu J. 2017. Dissecting genetic architecture of startle response in *Drosophila melanogaster* using
912 multi-omics information. *Sci Rep* 7. doi:10.1038/s41598-017-11676-1

913 Yang J, Benyamin B, McEvoy BP, Gordon S, Henders AK, Nyholt DR, Madden PA, Heath AC, Martin NG,
914 Montgomery GW, Goddard ME, Visscher PM. 2010. Common SNPs explain a large proportion of the
915 heritability for human height. *Nat Genet.* doi:10.1038/ng.608

916 Yang J, Manolio TA, Pasquale LR, Boerwinkle E, Caporaso N, Cunningham JM, De Andrade M, Feenstra B,
917 Feingold E, Hayes MG, Hill WG, Landi MT, Alonso A, Lettre G, Lin P, Ling H, Lowe W, Mathias RA,
918 Melbye M, Pugh E, Cornelis MC, Weir BS, Goddard ME, Visscher PM. 2011. Genome partitioning of genetic
919 variation for complex traits using common SNPs. *Nat Genet.* doi:10.1038/ng.823

920 Zeh JA, Bonilla MM, Adrian AJ, Mesfin S, Zeh DW. 2012. From father to son: Transgenerational effect of
921 tetracycline on sperm viability. *Sci Rep* 2. doi:10.1038/srep00375

922 Zhou S, Morozova T V., Hussain YN, Luoma SE, McCoy L, Yamamoto A, MacKay TFC, Anholt RRH. 2016. The
923 genetic basis for variation in sensitivity to lead toxicity in *drosophila melanogaster*. *Environ Health Perspect*
924 **124**:1062–1070. doi:10.1289/ehp.1510513

925 Zhou X, Stephens M. 2012. Genome-wide efficient mixed-model analysis for association studies. *Nat Genet* **44**:821–
926 824. doi:10.1038/ng.2310

927

Figure 3 – figure supplement 1 Comparison of pupation height status between *Wolbachia*-free and *Wolbachia*-infected stocks

# of stocks tested		Measurement statistics		Average Pupation height (mm)	Wilcox rank test (P-value)
		Vial	Individual		
Wolbachia free	93	# vials measured = 766 Mean replicates per IL= 8.2 ± 1.7 SD	Number of pupae measured = 31030; Mean replicates per IL= 333.7 ± 126.1 SD	29.9 ± 7.4 SD	0.3
Wolbachia infection	105	# vials measured = 861 Mean replicates per IL= 8.2 ± 1.6 SD	Number of pupae measured = 35373; Mean replicates per IL= 336.9 ± 106.6 SD	28.6 ± 7.5 SD	

Figure 3 – figure supplement 2: Experimental test of Wolbachia infection effect on pupation height. The Wolbachia-infection status of randomly selected Wolbachia-infected (A) and Wolbachia-free (C) stocks were confirmed with standard agarose gel electrophoresis after PCR amplification. The comparison of pupation height for Wolbachia-infected stocks and Wolbachia-free stocks and those after tetracycline treatment are shown in (B) and (D), respectively. The significance P-values were computed with Wilcoxon rank test.

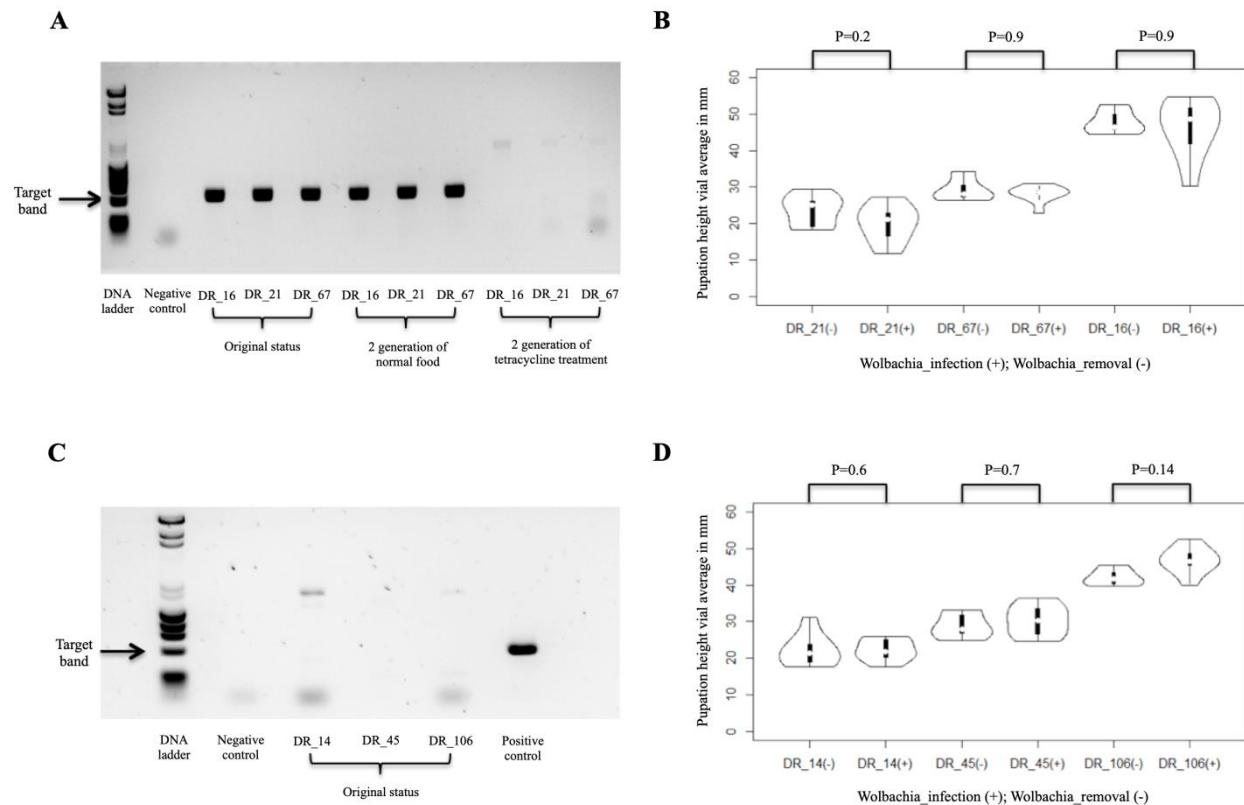
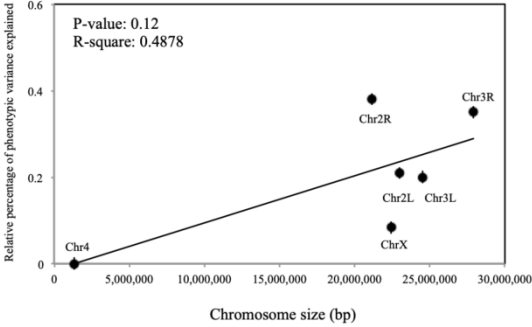
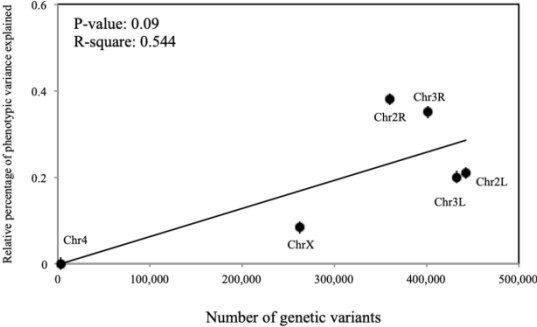


Table 1 - table supplement 1: Distribution of the explained phenotypic variance for each chromosome based on chromosome size for with (A) and without (C) chromosome 4, and number of genetic variants within each chromosome for with (B) and without chromosome 4 (D).

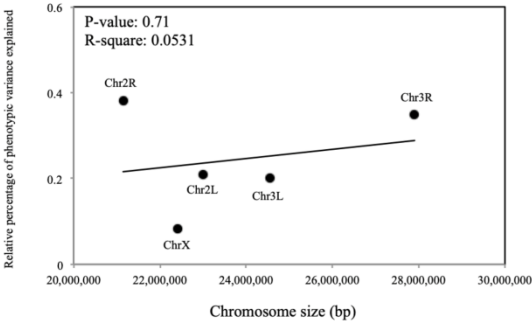
A



B



C



D

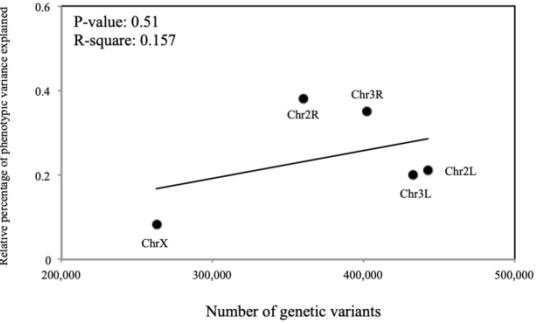


Figure 4 - figure supplement 1: Dependence of pupation height choice on pupal case size. (A) shows the correlation between pupae case length vial mean and pupation height vial mean, and the data was generated with all 1627 vial measurement from 198 DGRP strains; (B) shows the correlation of p-values between GWA on pupation height without covariate (x-axis) and that with pupae case length as covariate (y-axis); (C) and (D) show the Q-Q plots for genome-wide association results with pupation height as the trait for without covariate and that with pupae case length as covariate, respectively.

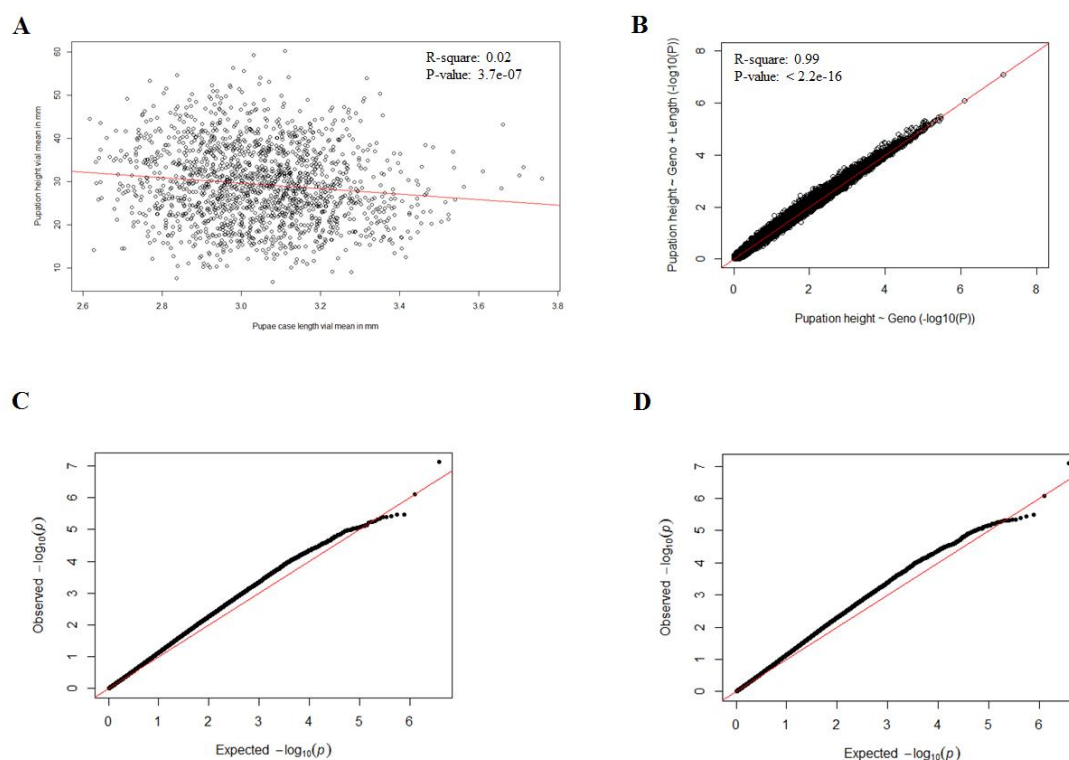


Figure 4 - figure supplement 2: Correlation between population structures and pupation height. The projections on the first and second PCs of genetic variant data are plotted for each DGRP strain. Strains were categorized into three equal-sized bins according to their pupation height (low - red, medium - blue, high - green).

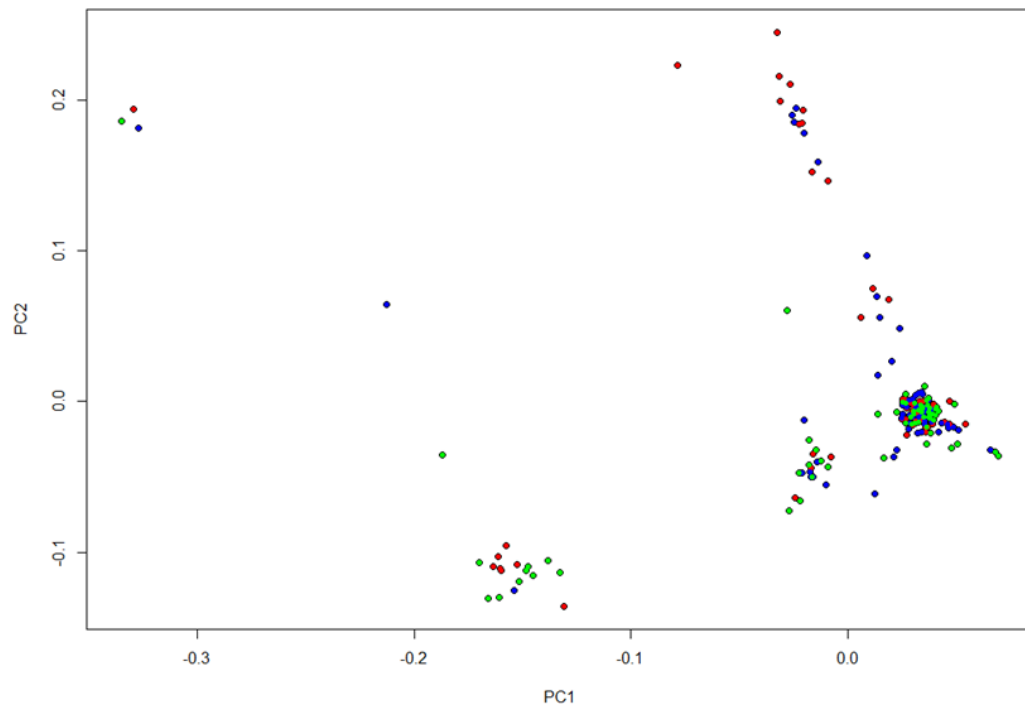


Figure 4 - figure supplement 3: Correlation between pupation height and top 20 PCs. The significance P-value and R-square were computed with linear regression model implemented in R platform.

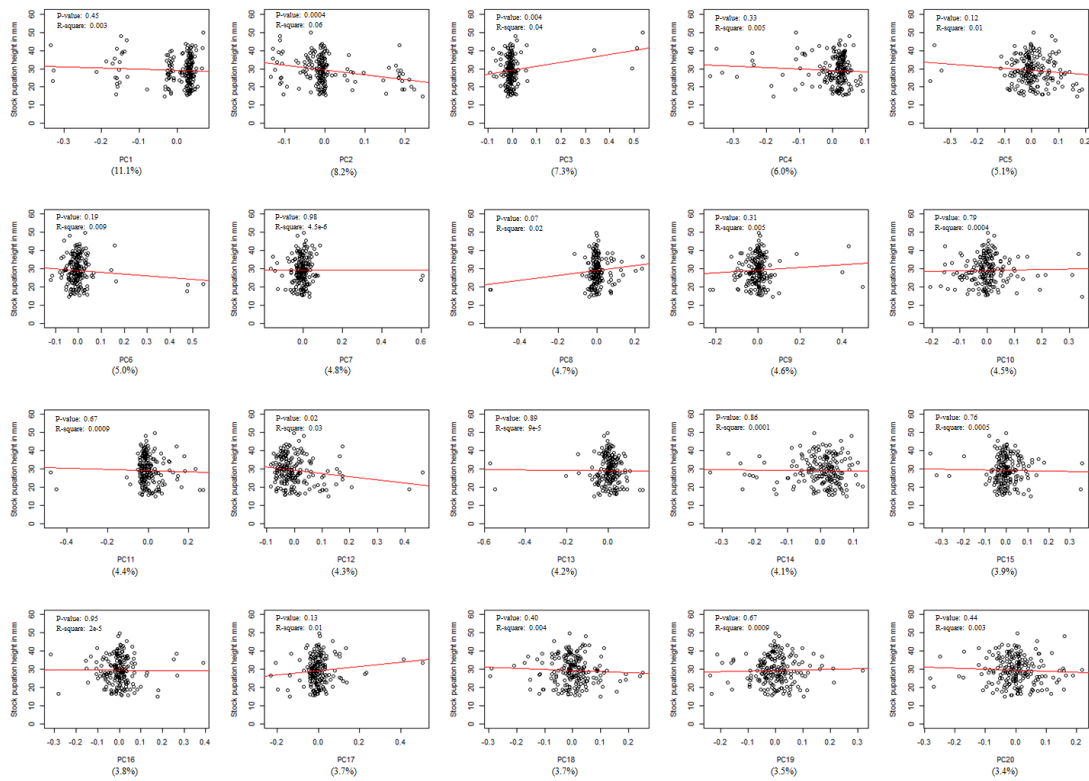


Figure 4 - figure supplement 4: Correlation between pupation height status and inversion status in DGRP strains. Significant p-values (< 0.05) are highlighted in red.

Inversion ID	Number of inbred strains			P-value (Pearson's correlation test)		
	No inversion	One inversion	Two inversion	VS PC1	VS PC2	VS pupation height
In(2L)t	155	25	18	< 2.2e-16	7.857e-06	0.07045
In(2R)NS	183	10	5	0.9927	0.8688	0.157
In(2R)Y1	197	1	0	0.6542	0.8424	0.07539
In(2R)Y2	197	1	0	0.8209	0.4832	0.5556
In(2R)Y3	197	1	0	0.7717	0.5068	0.7652
In(2R)Y4	197	1	0	0.7717	0.5068	0.7652
In(2R)Y5	197	1	0	0.5749	0.8693	0.6376
In(2R)Y6	198	0	0	NA	NA	NA
In(2R)Y7	198	0	0	NA	NA	NA
In(3L)P	194	2	2	0.6831	0.5733	0.6753
In(3L)M	197	1	0	0.6422	0.8501	0.4203
In(3L)Y	198	0	0	NA	NA	NA
In(3R)P	188	6	4	0.3478	0.4562	0.6713
In(3R)K	185	10	3	0.494	0.2189	0.5246
In(3R)Mo	172	9	17	3.62e-09	< 2.2e-16	0.05433
In(3R)C	196	2	0	0.6966	0.5922	0.1478

Table 2 - table supplement 1: LD regions for Genome-wide association results. The chromosomal coordinate for genetic variants are based on Flybase version 5.

Genetic variant	Variant coordinate (v5)	QTL region (v5)	Size (kb)	Genes
2L_2261132_SNP	2L:2261132	2L:2261132-2261165	0.033	CG4270
2R_4192787_SNP	2R:4192787	2R:4192787-4192809	0.022	CG30371/pdm3
2R_20001939_INS	2R:20001939	2R:20001420-20001945	0.525	CG4049,CG3253
3L_15604180_SNP	3L:15604180	3L:15604180-15604189	0.009	CG13449
3R_12465747_SNP	3R_12465747	3R:12435869-12476958	41.089	NPF,CG12873,CG10340,CG17562,CG17560,CG14893,CG14905,Fas1, nonA-I,Ar16IP1,CG10324,CCT3,CG14906,CG14907
3R_15464523_SNP	3R:15464523	3R:15464523-15464598	0.075	Subdued
3R_22219289_SNP	3R:22219289	3R:22216983-22227650	10.667	ppk15
3R_25643196_SNP	3R:25643196	3R:25643196-25643241	0.045	CG7829
3R_25865027_SNP	3R:25865027	3R:25864898-25865328	0.43	janA
X_12597625_SNP	X:12597625	X:12597591-12597661	0.07	Smr

Figure 8 – figure supplement 1: Comparison of pupation height GWA p-values and pupation height effect sizes (A) and pupae case length effect sizes (B) measured in gene homozygous disruption lines from transposon insertion mutagenesis. Each dot represents one gene disruption line. The pupation height GWA P-value was defined as the lowest p-value from all the genetic variants within the gene and the 5kb up/down-stream of target gene. Sig_Insertion_hm: homozygous transposon insertion lines for significant (GWA p-value <1E-05) associating genetic variants; Network_Insertion_hm: homozygous transposon insertion lines for genetic interaction network genes; Random_Insertion_hm: homozygous transposon insertion lines for random genes. The genes within blue rectangles are appearing as both significant GWA hits (P-value < 1.0E-05) and locating in the genetic interaction subnetwork.

